Modelling the life cycle dynamics of *Acartia clausi* - a key copepod species in the North Sea

Dissertation zur Erlangung des Doktorgrades
an der Fakultät für Mathematik, Informatik und Naturwissenschaften
Fachbereich Geowissenschaften
der Universität Hamburg

vorgelegt von

Chuanxi Xing
aus Yantai, China

Hamburg, 2013

-Korrigierte Fassung-

Tag der Disputation: 29 Oktober 2013

Als Dissertation angenommen vom Fachbereich Geowissenschaften
der Universität Hamburg

auf Grund der Gutachten von
Prof. Dr. Inga Hense
und Prof. Dr. Carsten Eden

Prof. Dr. Christian Betzler
Leiter des Fachbereichs Geowissenschaften

Abstract

Copepods play an important role in marine ecosystems, providing an important pathway for energy from primary producers to consumers at higher trophic levels. Changes in copepod abundance are observed, for instance, to affect the yields of commercially important fishes. Additionally, copepods are important for biogeochemical cycles, particularly the carbon cycle. A part of the carbon that is fixed by phytoplankton in the surface layers of the ocean and then ingested by copepods sinks rapidly into the deep ocean in the form of fecal pellets. It is assumed that environmental changes, in particular a rise in the sea temperature, will impact the life cycle dynamics of copepods. Copepods are very sensitive to temperature variations. Temperature variations can change the abundance of copepods directly through influencing their physiological processes and indirectly through the bottom-up effect by weakening or strengthening the temporal match between copepods and phytoplankton. Thus, concerns have been raised that future climate warming will affect the abundance of copepods through the direct and indirect effects.

In this thesis, I choose *Acartia clausi*, a key copepod species in the North Sea, as a representative of copepods. Through developing a life cycle model for *Acartia clausi* and coupling the developed model to a simple ecosystem model (including nutrient, phytoplankton, and detritus) and to the water column model GOTM, I study the life cycle dynamics of this species in the North Sea and project the potential responses of phytoplankton and *Acartia clausi* to projected North Sea temperature rises with a focus on the phenological changes.

I find that the ontogenetic development of *Acartia clausi* is more sensitive to variations in temperature and food concentration at lower temperatures than at higher temperatures. This result helps to better understand the observed mismatch between phytoplankton and *Acartia clausi* at the Stonehaven sampling station and implies that

future climate warming will greatly accelerate the development of *Acartia clausi* at the beginning of the growing season. I find that only the production of rapidly hatching subitaneous eggs should be considered in the life cycle model and the overwintering strategy of *Acartia clausi* in the North Sea is by adults. The seasonal cycle of *Acartia clausi* shows a marked seasonality in reproduction. In winter, due to low temperature and insufficient food supplies, the abundance of *Acartia clausi* is low and the reproductive activity of the overwintering adults ceases. In May, the overwintering adults begin to produce the first egg cohort when the increase in the phytoplankton biomass concentration can supply sufficient food. The adults produce eggs intensively and successively during the short breeding season from March to June. Several cohorts are produced during the short time and the developments of different cohorts overlap with each other. When most individuals of the first cohorts reach adulthood, the adult abundance reaches the annual maximum peak. From August onwards, the abundance of *Acartia clausi* begins to decrease due to the food deficiency.

In the warming scenario in which the annual mean sea surface temperature (SST) is increased by 1.2°C compared to the current level, the model results show that the higher temperature modifies the seasonalities of phytoplankton and *Acartia clausi*. Both the timings of the maximum phytoplankton biomass concentration peak and the first egg cohort from *Acartia clausi* are advanced by 8 days. Because the seasonal cycles of *Acartia clausi* and phytoplankton match more closely than under present environmental conditions, the abundance of *Acartia clausi* increases. In the warming scenarios in which the annual mean SST is increased by more than 2°C compared to the current level, the temporal match between *Acartia clausi* and phytoplankton is disturbed. The rising temperature increases the excretion rates of the overwintering adults, but at the same time the phytoplankton biomass concentration remains low due to the light limitation in winter. Because of the starvation, the abundance of overwintering adults decreases. The abundance of the overwintering stocks is an important factor determining the seasonal variation of *Acartia clausi* abundance. A severe reduction in the abundance of overwintering adults will lead to the situation that there will not be enough individuals to initialize the new seasonal cycle. Consequently, the abundance of *Acartia clausi* decreases sharply.

This study provides a comprehensive understanding of the life cycle dynamics of *Acartia clausi* in the North Sea and it is the first time that an estimate of the future

change in *Acartia clausi* abundance is given. Since *Acartia clausi* is an important food source for commercially important fishes, the knowledge obtained from this study is helpful for a better understanding of the mechanisms driving the food availability of fishes and is useful for developing a capacity to forecast the recruitment success of fishes in a warmer environment.

Zusammenfassung

Copepoden spielen eine wichtige Rolle in marinen Ökosystemen, indem sie Energie von den Primärproduzenten zu den Konsumenten der höheren trophischen Ebenen transferieren. Es wird beispielsweise beobachtet, dass Änderungen im Vorkommen von Copepoden die Erträge von kommerziell wichtigen Fischarten beeinflussen. Zusätzlich sind Copepoden wichtig für biogeochemische Zyklen, im Besonderen für den Kohlenstoffkreislauf. Ein Teil des Kohlenstoffs, der von Phytoplankton in den oberflächennahen Schichten des Ozeans gebunden und dann von Copepoden aufgenommen wird, sinkt in Form von Kotballen schnell in den tieferen Ozean. Man nimmt an, dass Umweltveränderungen und im Besonderen steigende Ozeantemperaturen die Lebenszyklusdynamik von Copepoden beeinträchtigen werden. Copepoden sind sehr sensitiv gegenüber Temperaturänderungen. Temperaturänderungen können das Vorkommen von Copepoden direkt durch Beeinflussen ihrer physiologischen Prozesse verändern, oder durch den bottom-up Effekt indem die zeitliche Übereinstimmung zwischen Copepoden und Phytoplankton geschwächt oder verstärkt wird. Aus diesen Gründen wurden Bedenken geäußert, dass eine zukünftige Klimaerwärmung das Vorkommen von Copepoden durch direkte und indirekte Effekte beeinflussen wird.

In dieser Arbeit wähle ich *Acartia clausi*, eine Schlüsselcopepodenart in der Nordsee, als typischen Vertreter von Copepoden. Indem ich ein Lebenszyklusmodell für *Acartia clausi* entwickele und dieses an ein einfaches Ökosystemmodell (welches Nährstoff, Phytoplankton und Detritus enthält) und ein physikalisches Modell koppele, untersuche ich die Lebenszyklusdynamik dieser Art in der Nordsee und projiziere die möglichen Reaktionen von Phytoplankton und *Acartia clausi* auf projizierte Temperaturen in der Nordsee in die Zukunft, wobei ich einen Fokus auf die phänologischen Veränderungen lege.

Es stellt sich heraus, dass die ontogenetische Entwicklung von *Acartia clausi* bei

niedrigen Temperaturen sensitiver gegenüber Temperaturschwankungen sowie Schwankungen im Nahrungsangebot reagiert als bei hohen Temperaturen. Dieses Ergebnis hilft den an der Probenstation Stonehaven beobachteten mismatch zwischen Phytoplankton und *Acartia clausi* zu verstehen und impliziert, dass eine zukünftige Klimaerwärmung die Entwicklung von *Acartia clausi* zu Beginn der Wachstumsperiode stark beschleunigen wird. Es zeigt sich, dass nur die Produktion von schnell schlüpfenden subitaneous Eiern [subitaneous eggs] im Lebenszyklusmodell berücksichtigt werden sollte und dass die Überwinterungsstrategie von *Acartia clausi* in der Nordsee durch die Adulten erfolgt. Der Jahreszyklus von *Acartia clausi* zeigt eine deutliche Saisonalität in der Fortpflanzung. Im Winter ist die Abundanz von *Acartia clausi* aufgrund niedriger Temperaturen und unzureichenden Nahrungsangebots niedrig und die Fortpflanzungsaktivität der überwinternden Adulten lässt nach. Im Mai beginnen die überwinternden Adulten die erste Kohorte Eier zu produzieren sobald der Anstieg der Phytoplanktonbiomassenkonzentration ausreichend Nahrungsangebot liefert. In der kurzen Brütezeit von März bis Juni produzieren die Adulten intensiv und fortlaufend Eier. Innerhalb kurzer Zeit werden mehrere Kohorten produziert und die Entwicklung der unterschiedlichen Kohorten überlappt. Sobald die meisten Individuen der ersten Kohorte ausgewachsen sind, erreicht die Abundanz der Adulten ihr Jahresmaximum. Ab August beginnt die Abundanz von *Acartia clausi* aufgrund von Nahrungsmangel abzunehmen.

Im Erwärmungsszenario, in dem die mittlere Ozeanoberflächentemperatur (SST) um 1.2°C gegenüber gegenwärtigen Werten erhöht ist, zeigen die Modellresultate, dass die höhere Temperatur die Saisonalität von Phytoplankton und von *Acartia clausi* verändert. Sowohl das Maximum der Phytoplanktonbiomassenkonzentration als auch die erste Kohorte an Eiern von *Acartia clausi* treten 8 Tage früher auf. Da die Jahreszyklen von *Acartia clausi* und Phytoplankton zeitlich besser übereinstimmen als unter gegenwärtigen Umweltbedingungen, steigt die Abundanz von *Acartia clausi* an. Im Erwärmungsszenario, in dem die jährlich gemittelte SST um mehr als 2°C gegenüber gegenwärtigen Werten erhöht ist, wird die zeitliche Übereinstimmung zwischen *Acartia clausi* und Phytoplankton gestört. Die steigenden Temperaturen erhöhen die Exkretionsraten der überwinternden Adulten, zugleich bleibt jedoch die Phytoplanktonbiomassekonzentration aufgrund der winterlichen Lichtlimitierung niedrig. Da die überwinternden Adulten verhungern, nimmt ihre Abundanz ab. Die Abundanz des überwinternden Bestandes ist ein wichtiger Faktor bei der Bestimmung der saisonalen Schwankung der *Acartia clausi* Abundanz. Eine starke Abnahme der Abundanz der

überwinternden Adulten wird zu einer Situation führen, in der es nicht ausreichend Individuen geben wird um den neuen Jahreszyklus in Gang zu setzen. Folglich nimmt die Abundanz von *Acartia clausi* stark ab.

Diese Untersuchung liefert ein umfassendes Verständnis der Lebenszyklusdynamik von *Acartia clausi* in der Nordsee und erstmals wird eine Einschätzung der zukünftigen Änderungen der *Acartia clausi* Abundanz getroffen. Da *Acartia clausi* eine wichtige Nahrungsquelle für kommerziell wichtige Fischarten darstellt, ist das aus dieser Arbeit entstehende Wissen für ein besseres Verständnis der Mechanismen, die das Nahrungsangebot von Fischen steuern, hilfreich und für die Entwicklung von Vorhersagemöglichkeiten des Vermehrungserfolgs von Fischen in einer wärmeren Umwelt nützlich.

Contents

Chapter 1

Introduction

1.1 Motivation

Copepods are a group of crustaceans. They form an important group of zooplankton and are probably the most numerous multicellular organisms on Earth (Mauchline, 1998). Copepods play an important role in many marine ecosystems as grazers, providing an important pathway for energy from primary producers to consumers at higher trophic levels, such as fishes and marine mammals. Changes in copepod abundance are observed to affect the abundance of different fish species and induce regime shifts in marine ecosystems. For example, climate variation induced changes in the abundance of *Acartia spp.* and *Pseudocalanus spp.* in the Baltic Sea caused a shift in the dominance of sprat and cod (Alheit et al., 2005; Möllmann et al., 2008). In the North Sea, the reduction in the abundance of *Calanus finmarchicus* greatly reduced the recruitment success of Atlantic cod (Beaugrand et al., 2003). These studies indicate that the abundance of copepods is an important factor influencing the survival of fishes. Copepods are additionally assumed to play an important role in biogeochemical cycles, in particular the carbon cycle (Ducklow et al., 2001). A part of the carbon that is fixed by phytoplankton in the surface layer and then ingested by copepods is rapidly transported into the deeper ocean through sinking of fecal pellets. This part of carbon can thus be removed from the atmosphere for a long time period (>hundreds of years). An increase or a decrease in the abundance of copepods will also affect the carbon export.

Changes in copepod abundance are reported to be correlated with changes in temperature (e.g., Planque and Fromentin, 1996; Reid et al., 2003). Directly, temperature variations can change the copepod abundance through influencing their physiological processes, such as the ingestion and the metabolism. The direct effects of the temperature on copepods are well illustrated in previous studies (e.g., McLaren, 1978; Huntley and Lopez, 1992). Indirectly, temperature variations can change the copepod abundance through the bottom-up effect. The seasonal development of copepod abundance depends on the temporal match between copepods and their food source: phytoplankton. Phenology, or the life cycle dynamics of plankton (zooplankton and phytoplankton), is very sensitive to climate variations because temperature is a key parameter affecting the growth rate, body size and generation time of plankton. Phenological changes of zooplankton and phytoplankton due to climate variations have been observed in different marine ecosystems. In the subarctic North Pacific, for example, the timing of the annual maximum biomass peak of *Neocalanus plumchrus* has shifted dramatically between 1956 and 1998 (Mackas et al., 1998). In warm years (in the 1990s) the timing of the maximum *Neocalanus plumchrus* biomass peak is 1.5 to 2 months earlier than that in cold years (in the 1970s). The climate variation induced shifts in the seasonality of plankton in the North Sea were reported in Edwards and Richardson (2004).

The energy balance of the climate system is disturbed by the increased atmospheric concentration of greenhouse gases, which leads to a rapid warming of the atmosphere and ocean (IPCC, 2007). From the mid-1950s to the mid-1990s, the mean sea temperature in the upper 300 m of the global oceans has been increased by 0.31°C (Levitus et al., 2000). Because the situation that humans rely on fossil fuel as the main energy source has not been changed, it is projected that in the future the warming trend of oceans will continue. Future climate warming will have substantial impacts on copepod communities (Richardson, 2008). One aspect is that the climate warming will change the physiological processes of copepods and further cause a change in copepod abundance. Another aspect is that copepods and phytoplankton might fail to response to climate warming synchronously, which may cause a temporal mismatch between them. The decoupling of the phenological relation might cause a decline in copepod abundance. The concerns about changes in the copepod abundance is that the signal will resonate to upper trophic levels, affecting the yields of commercially important fishes.

In this thesis, I choose *Acartia clausi*, a key copepod species in the North Sea as a representative of copepods. Through modelling the life cycle dynamics of this species, I want to get a better understanding about how climate warming will influence copepods, directly and indirectly.

1.2 North Sea ecosystem

I focus on the North Sea for several reasons. Firstly, the North Sea is a biologically rich and productive region. Studying the North Sea ecosystem is of significant biological meaning. Secondly, the observations of the North Sea ecosystem are numerous. These observations provide a good knowledge about the foodwebs and copepod communities. Following, I will briefly introduce the ecosystem of the North Sea.

Hydrography The North Sea is a shallow marginal sea of the North Atlantic Ocean. From the south to the north, the bottom depth of the North Sea increases gradually from less than 30 m to 200 m (De Wilde et al., 1992). Strong westerly winds, the inflow of the North Atlantic water as well as strong tidal currents work together and lead to a complicated hydrographical structure (De Wilde et al., 1992). The basic ocean circulation pattern in the North Sea is cyclonic (Turrell et al., 1992). The mean residence time of the water in different parts of the North Sea ranges between 1 and 2 years (Eisma, 1987).

There are roughly three main water masses in the North Sea: the North Atlantic water mass, the continental coastal water mass and the mixed central North Sea water mass (Otto et al., 1990). The North Atlantic water, entering from the north through the Shetland-Orkney region and from the south through the English Channel, forms the North Atlantic water mass. The North Atlantic water mass is characterized by clear water with high salinity, moderate temperature. The climatological monthly mean SST in the regions where the North Atlantic water mass dominates is 6-8°C in winter and 12-14°C in summer. The water with low salinity, high nutrient concentration from the continental coasts and the Baltic Sea forms the continental coastal water mass. The climatological monthly mean SST in the regions where continental coastal water mass dominates is 2-4°C in winter and 17-19°C in summer. The North Atlantic water mass and the continental coastal water mass mix in the North Sea and form the mixed central

North Sea water mass. The climatological monthly mean SST in the central North Sea is 5-6°C in winter and 13-16°C in summer.

Stratification of the water column is a significant hydrographical character in the North Sea (De Wilde et al., 1992). The formation of the temporal thermostratification due to the solar heating of the upper water layers in summer is common in the north and central North Sea but in the shallow south North Sea, strong tidal mixing prevents the stratification of the water column (Otto et al., 1990).

Trophic levels A variety of organisms, commonly grouped as microbes, phytoplankton, zooplankton, benthos, fish, marine mammals and sea birds form the biota of the North Sea. The interactions and trophic relations between these organisms are extremely complex. The classic diagram of the trophic relations of these organisms in the North Sea is that phytoplankton production supplies energy for herbivorous zooplankton, herbivorous zooplankton serve as a major food source for higher trophic levels, and the detritus from phytoplankton, zooplankton and organisms of the higher trophic levels is the food source for the benthic system (Steele, 1974). The North Sea can be divided into three subregions (southern, central and northern) by the 50, 100 m contour lines based on the physical environments such as temperature and the stability of the water column (De Wilde et al., 1992) as well as the general distribution patterns of phytoplankton (Reid et al., 1990) and zooplankton (Fransz et al., 1991). In the following, I will introduce briefly the first and the second trophic levels.

Phytoplankton production from photosynthesis in the surface layer is the main energy source for the North Sea ecosystem. In the three subregions of the North Sea, the amount of net phytoplankton production that is available for heterotrophs is different (De Wilde et al., 1992). In the southern North Sea, the annually averaged value is 200 g C m^{-2}, in the central North Sea, the value is 250 g C m^{-2} and in the northern North Sea, the value is 100-200 g C m^{-2} (Reid et al., 1990). Two types of phytoplankton production are generally distinguished: bloom production (diatoms, due to high nitrate levels) occurring in early summer and regenerated production (flagellates, due to high ammonia levels) occurring later in the year (Smetacek, 1984).

Phytoplankton production sustains a large abundance of zooplankton. Herbivorous copepods form the major portion of zooplankton (Fransz et al., 1998; Nielsen and Munk, 1998), contributing substantially to the diet of fishes (Nielsen and Munk, 1998).

The main part of the copepod stocks is composed by three most commonly occurring groups: *Acartia spp.*, *Pseudocalanus elongatus* and *Calanus finmarchicus* (Fransz et al., 1991).

Calanus finmarchicus is a large sized copepod species and is most commonly found in the oceanic regions (Fransz et al., 1991). The persistence of its population in the North Sea depends heavily on the replenishment by oceanic influx (Glover, 1957). Because of the change in the North Sea temperature, the abundance of *Calanus finmarchicus* is decreasing (Beaugrand et al., 2003). *Pseudocalanus elongatus* is a copepod species that lives in both oceanic and coastal regions. It is regarded as one of the most typical copepod species in the North Sea (Rae and Rees, 1947).

Acartia spp. is a group of copepod species belonging to the genus *Acartia*. Several species of this genus can be found in the North Sea: *Acartia clausi*, *Acartia discaudata*, *Acartia bifilosa* and *Acartia tonsa* (Fransz et al., 1991). The latter three species are considered as brackish water species, which are rare in the open North Sea and generally accumulate in the estuaries. *Acartia clausi* is the largest species in body size in this genus (Bradford, 1976). It does not resident in waters with low salinity. In the North Sea, *Acartia clausi* is widely distributed and has a considerable abundance. In the northwestern North Sea along the Scottish coast, *Acartia clausi* was observed to dominate the local zooplankton abundance in most of the observation years (Lindley et al., 1995).

Research focus I focus on *Acartia clausi* for several reasons. Firstly, *Acartia spp.* is one of the dominant copepod groups in the North Sea. Studying the life cycle dynamics of one species from this copepod group is meaningful. Secondly, *Acartia clausi* is widely distributed in temperate waters and is a food source for commercially important fishes (Porumb, 1973). Knowledge of *Acartia clausi* can be applied to better understand the mechanism driving the food availability of fishes. Thirdly, the role of *Acartia clausi* played in North Sea ecosystems might become more and more important in the future because in the Baltic Sea, *Acartia spp.* were observed to become more abundant when sea temperature rises (Möllmann et al., 2008).

In this thesis, I model the life cycle dynamics of *Acartia clausi* and project the responses of this species to future climate warming with a focus on changes in its phenology and abundance. In particular, I am interested in the question whether the

temporal synchrony between the seasonal cycle of *Acartia clausi* and phytoplankton will be disturbed by future climate warming. I study the responses of *Acartia clausi* to climate warming by taking into account the life cycle dynamics because climate warming impacts zooplankton through changing their important biological processes and some of the biological processes occur only in specific life cycle stages.

1.3 Research aims

I conduct the research in two steps. In the first step, I study the life cycle dynamics of *Acartia clausi* in the North Sea. In the second step, I project the potential responses of phytoplankton and *Acartia clausi* to projected North Sea temperature rises.

Specifically, I want to address the following questions:

- How is the sensitivity of the ontogenetic development of *Acartia clausi* to the variations in the temperature and food concentration at different temperature conditions?
- Which reproductive pattern can best explain the observed seasonal variation of *Acartia clausi* abundance and which kind of overwintering strategy of *Acartia clausi* should be considered when modelling the life cycle dynamics of this species in the North Sea?
- How does the life cycle dynamics of *Acartia clausi* look like in the North Sea?
- What are the potential responses of phytoplankton and *Acartia clausi* to future climate warming? And what are the mechanisms behind?

1.4 Thesis outline

In Chapter 2, I introduce the observed seasonal variations of SST, the chlorophyll concentration and *Acartia clausi* abundance at the Stonehaven sampling station.

In Chapter 3, I develop a life cycle model for *Acartia clausi* to study the sensitivity of the ontogenetic development of *Acartia clausi* to the variations in the temperature and food concentration at different temperature conditions.

In Chapter 4, I model the seasonal variation of *Acartia clausi* abundance under different reproductive patterns and I discuss which kind of the reproductive pattern should be considered when modelling the life cycle dynamics of *Acartia clausi* and what is the possible overwintering strategy of this species in the North Sea.

In Chapter 5, I study the life cycle dynamics of *Acartia clausi* in the North Sea and project the potential responses of *Acartia clausi* and phytoplankton to future climate warming.

In Chapter 6, I summarize the whole thesis and propose the next steps in observational studies and model applications.

Chapter 2

Observations at the Stonehaven sampling station

2.1 Introduction

The Stonehaven sampling station locates in the northwestern North Sea (Figure 2.1). The water depth at this station is 48 m. An introduction to the hydrographical conditions at the Stonehaven sampling station is available in Bresnan et al. (2009) and Bresnan (2012).

Hydrographic parameters, nutrient concentrations, and the abundances of phytoplankton and zooplankton species have been measured weekly (if weather conditions allow, 47 times per year on average) at the Stonehaven sampling station since January 1997. The long time series and high temporal resolution observations provide an insight into the seasonal cycle of the phytoplankton and zooplankton species. The SST data, surface chlorophyll α concentration data (in mg chl m^{-3}, in the following called the chlorophyll concentration) and vertically integrated *Acartia clausi* abundance (in individuals m^{-2}, covering the two life cycle stages: copepodite and adult) data measured during the period from 1999 to 2010 are available for this thesis. The data are provided by Dr. Eileen Bresnan and Ms Tracy McCollin from Fisheries Research Services Marine Laboratory, Aberdeen, UK under the Open Government Licence (Open Government Licence, 2013).

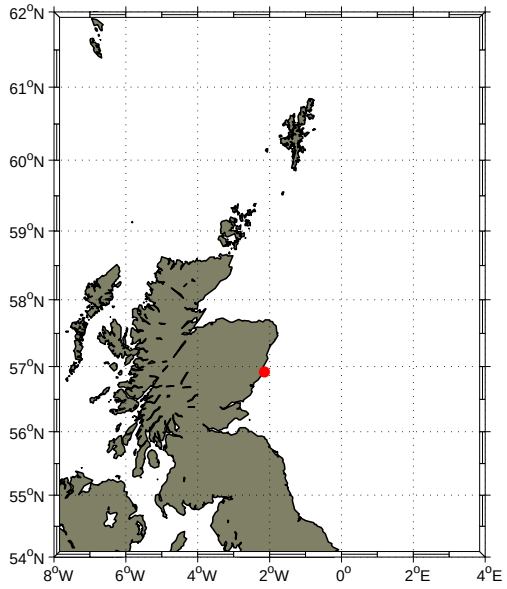

Figure 2.1: The location of the Stonehaven sampling station (red dot, coordinate: 56°57.8'N, 02°06.2'W).

2.2 Analysis methods

The seasonal variations of SST, chlorophyll concentration and *Acartia clausi* abundance show strong interannual variabilities. The timing of the maximum chlorophyll concentration peak and *Acartia clausi* abundance peak, and the extents of their growing seasons are different from year to year. In order to display the observation data, I use the non-parametric analysis method box-and-whisker plot (McGill et al., 1978). The bottom and top of the filled box are the first and third quartiles. The tips of the upper and lower whiskers mean the lowest datum that is still within 1.5 interquartile range of the lower quartile, and the highest datum that is still within 1.5 interquartile range of the upper quartile, respectively. The circles mean the median values and the crosses mean outlier values that can not be included between the whiskers.

The climatological mean timing and amplitude of the maximum chlorophyll concentration peak and *Acartia clausi* abundance peak are defined in several steps. Taking the chlorophyll concentration for example, the process is that firstly the timing and amplitude of the maximum chlorophyll concentration peak of each individual year are defined. Then, I average the timing of each observation year as the climatological mean

timing and average the amplitude of each observation year as the climatological mean amplitude. The same process is applied to *Acartia clausi* abundance.

2.3 Results

Sea surface temperature There is a strong interannual variability in the seasonal variation of SST. But the general seasonal pattern is similar for all years: the annual minimum SST occurs, on average, in late February/early March with the value of around 6°C, and the annual maximum SST occurs in August/September with the value of 12-14°C (Figure 2.2). The annual mean SST at the Stonehaven sampling station during the observation period is 9.6°C.

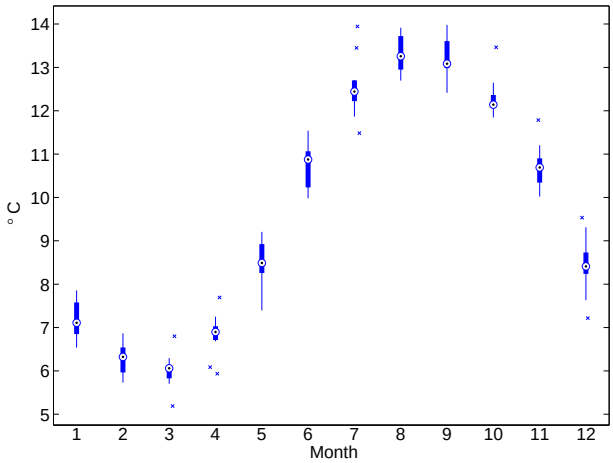

Figure 2.2: The monthly mean SST from 1999-2010 at the Stonehaven sampling station.

Chlorophyll concentration The seasonal variation of the chlorophyll concentration and the climatological mean timing and amplitude of the maximum chlorophyll concentration peak are shown in Figure 2.3a. The chlorophyll concentration at the Stonehaven sampling station is characterized by an apparent spring bloom. High chlorophyll concentrations are recorded from week 15 to week 25 with values ranging from 2 to 3 mg chl m^{-3} (median values). The climatological mean timing of the chlorophyll concentration peak is in week 21 at a level of 5.7 mg chl m^{-3}. From week 26, the chlorophyll concentration begins to decrease gradually but the value is still above 1 mg chl m^{-3} (median values). After week 40, the value of the chlorophyll concentration is below 1

mg chl m^{-3}. At the beginning of the year, the chlorophyll concentration can reach 1 mg chl m^{-3} after week 12. Before week 12, the chlorophyll concentration remains at a low level.

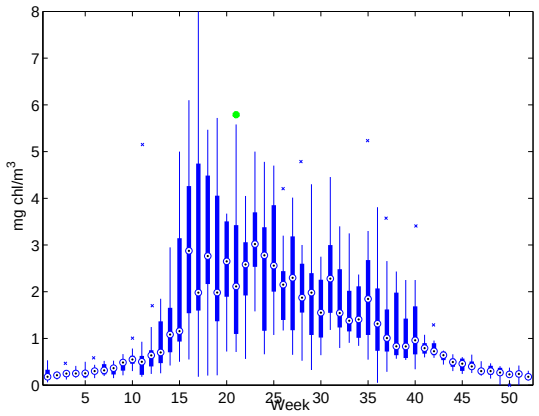

(a)

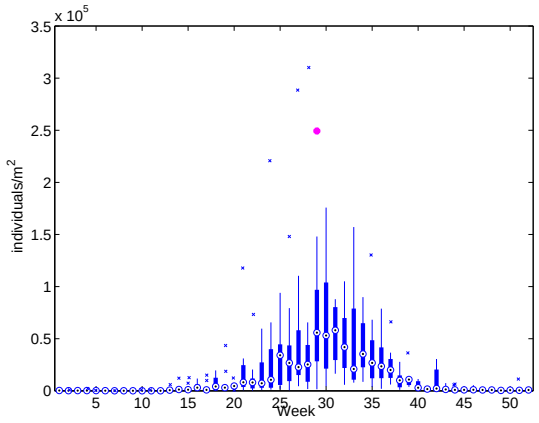

(b)

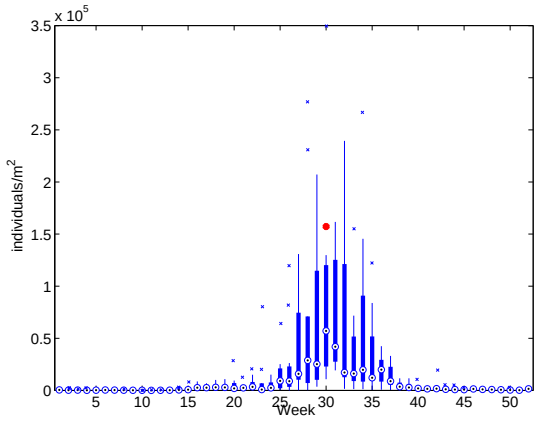

(c)

Figure 2.3: Weekly mean of the surface chlorophyll concentration (a), the vertically integrated copepodite abundance (b), the vertically integrated adult abundance (c) from 1999-2010. Additionally shown are: the climatological mean timing and amplitude of the maximum surface chlorophyll concentration peak in (a), green dot; the maximum vertically integrated copepodite abundance peak in (b), magenta dot; the maximum vertically integrated adult abundance peak (c), red dot.

***Acartia clausi* abundance** The seasonal variations of the copepodite and adult abundance, and the climatological mean timing and amplitude of the maximum copepodite and adult abundance peak are shown in Figure 2.3b, c. The high copepodite abundance is recorded from week 23 to week 36. During this period, it is possible for the value of copepodite abundance to be higher than 0.5×10^5 individuals m^{-2}. The climatological mean timing of the maximum copepodite abundance peak is in week 29. The climatological mean amplitude of the maximum copepodite abundance peak is 2.5×10^5 individuals m^{-2}. From the beginning of the year to week 20 and from week 40 to the end of the year, the copepodite abundance remains low.

The high adult abundance is recorded from week 27 to week 35. During this period, the adult abundance can reach higher than 0.5×10^5 individuals m^{-2}. The climatological mean timing of the adult abundance peak is in week 30. The climatological mean amplitude of the maximum adult abundance peak is 1.5×10^5 individuals m^{-2}. From beginning of the year to week 24 and from week 36 to the end of the year, the adult abundance remains at a low level.

Interpretation of the dataset There is an apparent temporal mismatch between the seasonal variations of the chlorophyll concentration and *Acartia clausi* abundance. The *Acartia clausi* copepodite and adult abundance increase after the high chlorophyll concentration. In order to better illustrate this feature, I normalize the chlorophyll concentration of each year by dividing the seasonal variation of the chlorophyll concentration of each year with its own amplitude of the maximum peak. By doing this, I intend to exclude the noises caused by the interannual variability in the chlorophyll concentration. I also normalize the copepodite abundance with the same method. The results are shown in Figure 2.4. The earliest timing of the maximum chlorophyll concentration peak at the Stonehaven sampling station during the observation period is in week 15 (beginning of March). But for *Acartia clausi*, before week 21 (end of April) there is hardly any chance that the copepodite abundance can reach 10% of the amplitude of its maximum peak. This indicates that there is a time lag of about 6 weeks between the maximum chlorophyll concentration and the initialization of the seasonal variation of *Acartia clausi* abundance.

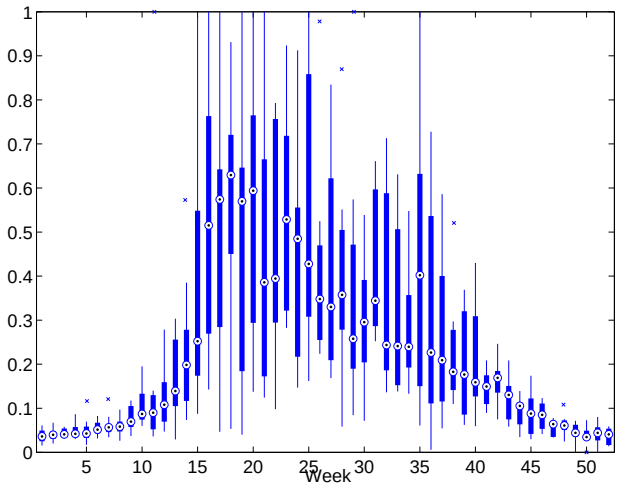

(a)

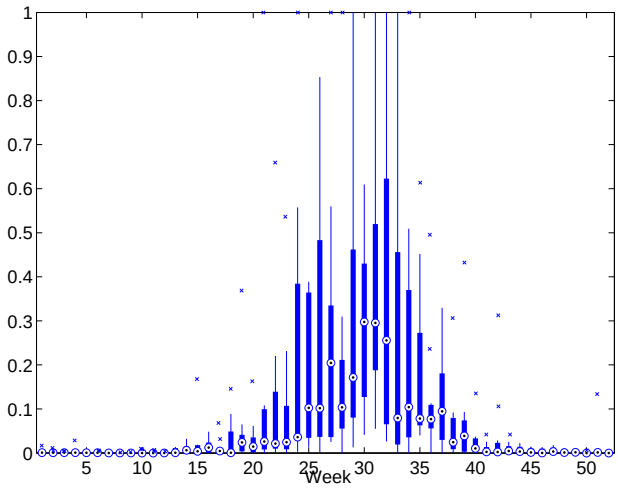

(b)

Figure 2.4: The normalized seasonal variations of the chlorophyll concentration (a) and *Acartia clausi* copepodite abundance (b)

Chapter 3

Influences of temperature and food concentration on the ontogenetic development of *Acartia clausi*

3.1 Motivation

In order to project the impact of the climate variation on copepods, the effects of the environmental factors on the ontogenetic development of copepods have to be considered. Temperature and food availability are the main environmental factors determining the development of copepods. The effect of temperature on the development of copepods has been well described in previous studies. Huntley and Lopez (1992) analyzed the growth rates of 33 copepod species and suggested that temperature alone could explain more than 90% of the variations in their growth rates. But there are also some studies showing that the copepod development is often limited by food availability. For example, in the North Sea, the growth rates of copepods were found to decrease in summer when the food availability was deficient (Klein Breteler and Gonzalez, 1982). In the Dutch Oosterschelde estuary, it was observed that the development rates of *Acartia clausi* and *Temora longicornis* were reduced during summer (Bakker et al., 1988). From these studies, it seems that the influences of the two factors on the development of copepods vary in different situations.

In this chapter, I develop a life cycle model for *Acartia clausi* and simulate its development time from egg to adult in different environmental conditions. With this model, I also conduct sensitivity experiments to study the sensitivity of the development of *Acartia clausi* to variations in the temperature and food concentration at different temperature conditions. By doing this, I aim to get a better understanding of the observed time lag between the seasonal variations of the chlorophyll concentration and *Acartia clausi* abundance at the Stonehaven sampling station.

3.2 *Acartia clausi* life cycle model

There are already some studies about modelling the development of copepods. A life cycle model for *Pseudocalanus spp.* in the Baltic Sea was established by Fennel (2001). The model simulated the life cycle of *Pseudocalanus spp.* by resolving both the biomass and abundance of five ontogenetic life cycle stages. An advantage of this kind of model is that biological processes are described for each life cycle stage so that the effects of the environmental conditions on the life cycle dynamics of copepods can be considered. Based on the basic model structure from Fennel (2001), Stegert et al. (2007) introduced new parametrizations for some biological processes and calibrated a life cycle model for *Pseudocalanus elongatus* in the North Sea. These model studies provided a good opportunity to get a better understanding of the life cycle dynamics of copepods when in situ observations which cover the whole copepod life cycle were absent.

The structure of the current *Acartia clausi* life cycle model is adopted from Fennel (2001). The biological processes of *Acartia clausi* are parametrized according to the information published in literature. The parameter values which are difficult or impossible to obtain from the previous studies are estimated with the laboratory experimental data from Klein Breteler and Schogt (1994). Here, I first introduce the model structure and parametrizations of different biological processes. The dataset and the estimation of the uncertain parameter values are introduced later.

3.2.1 Equation system

The life cycle of *Acartia clausi* is composed of 13 life cycle stages: egg, nauplius (NI-NVI), copepodite (CI-CV), adult (CVI). In the model, I simplify this life cycle into four life cycle stages because in the observations, one generally regards the life cycle stages with similar morphological characters and behaviors as one 'integrated' life cycle stage. The life cycle model of *Acartia clausi* adopts four life cycle stages: egg, nauplius, copepodite, adult. For convenience, I label them as i=1, 2, 3, 4, respectively. For each life cycle stage the biomass $\left[\vec{Z} = (Z_1, Z_2, Z_3, Z_4)\right]$ (in mmol N m^{-3}) and abundance $\left[\vec{A} = (A_1, A_2, A_3, A_4)\right]$ (in individuals m^{-3}) are resolved. The prognostic equations (equation 3.1) of the model are as follows:

$$\begin{aligned} \frac{\partial \vec{Z}}{\partial t} &= \mathbf{M_Z}\vec{Z}' \\ \frac{\partial \vec{A}}{\partial t} &= \mathbf{M_A}\vec{A}' \quad , \end{aligned} \tag{3.1}$$

where the non-linear matrices (M_Z and M_A) are:

$$\mathbf{M_Z} = \begin{pmatrix} \psi_1 - \tau_{1,2} & 0 & 0 & 0 \\ +\tau_{1,2} & \psi_2 - \tau_{2,3} & 0 & 0 \\ 0 & +\tau_{2,3} & \psi_3 - \tau_{3,4} & 0 \\ 0 & 0 & +\tau_{3,4} & \psi_4 \end{pmatrix} ,$$

$$\mathbf{M_A} = \begin{pmatrix} \phi_1 - \tau_{1,2} & 0 & 0 & 0 \\ +\tau_{1,2} & \phi_2 - \tau_{2,3} & 0 & 0 \\ 0 & +\tau_{2,3} & \phi_3 - \tau_{3,4} & 0 \\ 0 & 0 & +\tau_{3,4} & \phi_4 \end{pmatrix} .$$

In the non-linear matrices, the term $\psi_i = (g_{i_P} + g_{i_{D_s}}) - l_i - \eta_i$ means the source terms or loss terms of the biomass: ingestion ($g_{i_P}, g_{i_{D_s}}$ when $i = 2, 3, 4$), egestion and excretion (l_i when $i = 2, 3, 4$), and mortality (η_i when $i = 1, 2, 3, 4$); the term $\phi_i = -\eta_i$ represents mortality (η_i when $i = 1, 2, 3, 4$), which is the loss term of the abundance. In the non-linear matrices, the life cycle stage transition rates ($\tau_{i,j} = \iota_{i,j}$ or $\kappa_{i,j}$) represent hatching ($\iota_{1,2}$) or moulting ($\kappa_{2,3}$ or $\kappa_{3,4}$). Note that in this chapter, I do not consider the reproduction of adult. I model only the development from egg to adult. The reproduction of adult is introduced and discussed in Chapter 4.

3.2.2 Parametrizations of biological processes

The parametrizations of ingestion, life cycle stage transition, egestion and excretion, mortality are introduced in the following sections. During my introduction of the parametrizations of these biological processes, I also introduce how I choose the values of some parameters and provide references.

3.2.2.1 Ingestion

Ingestion is the most important biological process that determines the development time. *Acartia* species are omnivorous (Hu et al., 2012). *Acartia clausi* feeds on phytoplankton as well as on small detritus (slowly sinking dead organic matters) (Uye, 1981; Mayzaud et al., 1998). I use the terms D_s and P to present the two food sources: small detritus and phytoplankton. The ingestion rate (g_i) is calculated with equation:

$$\begin{aligned} g_i &= g_{i_P} + g_{i_{D_s}} \\ g_{i_P} &= g_{i_{\max_P}} f_1(P)\ f_2(T)\ f_3(W)\ \frac{P}{P+D_s} \\ g_{i_{D_s}} &= g_{i_{\max_D}} f_1(D_s)\ f_2(T)\ f_3(W)\ \frac{D_s}{P+D_s} \quad . \end{aligned} \tag{3.2}$$

In Equation 3.2, the ingestion rates (g_{i_P} and $g_{i_{D_s}}$, for i=2,3,4) that describe the amount of food ingested per day are influenced by three factors: the food concentration ($f_1(P)$, $f_1(D_s)$), temperature ($f_2(T)$) and the individual body weight ($f_3(W)$). The terms $g_{i_{\max_P}}$ and $g_{i_{\max_D}}$ are the maximum grazing rates on phytoplankton and detritus.

Following, I will first introduce how I choose the values for $g_{i_{\max_P}}$ and $g_{i_{\max_D}}$ and then introduce the parametrizations of $f_1(P)$, $f_1(D_s)$, $f_2(T)$ and $f_3(W)$. The values of $g_{i_{\max_P}}$ and $g_{i_{\max_D}}$ are taken from previous observations. Katechakis et al. (2004) investigated the ingestion rate of *Acartia clausi* when it was fed with the saturated food concentration and measured the maximum ingestion rate to be 0.56±0.14 d^{-1}. This value agrees with the measurement of the ingestion rate of adult from another *Acartia* species (*Acartia tonsa*) in White and Roman (1992), in which the maximum ingestion rates for nauplius, copepodite and adult were measured to be 2.8 d^{-1}, 1.8 d^{-1} and 0.56 d^{-1} when *Acartia tonsa* was fed with the saturated food concentration. Because *Acartia clausi* and *Acartia tonsa* are genetically similar species, and both

observations were made under saturated food concentrations, I set the value of $g_{i_{\max_P}}$ (i=2,3,4) referring to White and Roman (1992). Small detritus is a food source of low quality. According to Mayzaud et al. (1998), the ingestion rate of *Acartia clausi* is higher when it was fed with small detritus than when it was fed with phytoplankton. But no actual values were measured in previous studies. In the model, I assume the values of $g_{i_{\max_D}}$ to be 2 times higher than the values of $g_{i_{\max_P}}$.

Food dependent ingestion Mayzaud et al. (1998) studied the ingestion of *Acartia clausi* under different food concentrations and found that the ingestion of this species followed a Holling type 2 (Holling, 1965) response to different food concentrations. In this model, the food dependent ingestion is calculated with following equation:

$$\begin{aligned} f_1(P) &= \frac{P^\alpha}{P^\alpha + k_P^\alpha} \\ f_1(D_s) &= \frac{D_s^\alpha}{D_s^\alpha + k_{D_s}^\alpha} \quad , \end{aligned} \tag{3.3}$$

where the terms k_P and k_{D_s} are the half saturation coefficients for phytoplankton and small detritus, and α is a curve factor. In Mayzaud et al. (1998), the value of the half saturation coefficient (k_P) for phytoplankton was measured to be ranging from 170 to 200 μg protein l^{-1}. If 16% of protein can be regarded as nitrogen (Geider and Roche, 2002) and using gram to mole conversion of nitrogen, the value of k_P then equals to 1.9-2.3 mmol N m^{-3}. Here, I set the value of k_P to be 2.3 mmol N m^{-3}. Mayzaud et al. (1998) also measured the half saturation coefficient for small detritus and found that when *Acartia clausi* was fed with small detritus, the ingestion rate increased linearly with the small detritus concentration without reaching a saturation. The reason was that the small detritus was a food source of low quality. In this model, I thus set the half saturation constant for small detritus (k_{D_s}) to be 2.5 times larger than that for phytoplankton (k_P). The value of the curve factor (α) is estimated with the observation data, I will come to this issue later.

Temperature dependent ingestion For the temperature dependent ingestion, a modified Gaussian function is used:

$$f_2(T) = \exp(-(\frac{T - T_{opt}}{T_1 - sign(T_2, T - T_{opt})})^2) \quad , \tag{3.4}$$

where the term T_{opt} is the optimum temperature for grazing, and T_1 and T_2 are two reference temperatures. The shape of Equation 3.4 is controlled by the values of T_1 and T_2. Direct measurements of the relation between temperature and the ingestion rate are rare. Instead, I use the relation between temperature and the egg production rate to estimate the temperature dependent ingestion because the egg production rate of copepods can be used to estimate ingestion conditions (Dagg, 1977). Sullivan and McManus (1986) investigated this relation and found the maximum egg production rate of *Acartia clausi* occurred at 15°C. In Uye (1981), the egg production rate of *Acartia clausi* under saturated food conditions was measured to be high at 14.7-17°C, all exceeding 60 eggs female d^{-1}. The two observations are quite close. Here, I set the value of T_{opt} to be 15°C following Sullivan and McManus (1986). The values of T_1 and T_2 are estimated with the observation data. I will come to this issue later.

Body weight dependent ingestion To parametrize the inhibition effect of cuticle of copepods on ingestion (this phenomenon was observed and reported in McLaren (1986)), I follow the model design from Stegert et al. (2007). A parabolic function is used:

$$f_3(W_i) = \begin{cases} 1 & \text{for} \quad W_i \leq W_{min_i} \\ 1 - \left(\frac{W_i - W_{min_i}}{W_{max_i} - W_{min_i}}\right)^2 & \text{for} \quad W_{min_i} < W_i \leq W_{max_i} \\ 0 & \text{for} \quad W_{max_i} < W_i \quad , \end{cases} \tag{3.5}$$

where the term W_i is the mean individual body weight, calculated as the ratio between the total biomass (Z_i) and the total abundance (A_i), the terms W_{min_i} and W_{max_i} are the minimum individual body weight and the maximum individual body weight. The values of W_{min_i} and W_{max_i} are listed in Table 3.1. Equation 3.5 controls that individuals are able to ingest at a maximum rate up to the minimum individual body weight (W_{min_i}), and when the mean individual body weight exceeds the minimum individual body weight, the ingestion rates decrease gradually down to zero at the maximum individual body weight (W_{max_i}).

3.2.2.2 Egestion and excretion

Egestion and excretion are two loss terms of the biomass. The ingested food is partly used for growth, and the rest is lost through egestion (faecal pellets) and metabolism.

In the model, I consider the egestion and excretion of nauplius, copepodite and adult (i=2,3,4).

Egestion Egestion is formulated as $(1-\beta_P)g_{i_P}+(1-\beta_{D_s})g_{i_{D_s}}$, where the terms β_P and β_{D_s} are the assimilation efficiencies for phytoplankton and small detritus. The value of β_P are given following Mayzaud et al. (1998). Mayzaud et al. (1998) observed that the assimilation efficiency for phytoplankton ranges from 0.76 to 0.78. In the model, I use the median value of 0.77 for β_P. About the value of β_{D_s}, there is no direct measurement. In Mayzaud et al. (1998), the assimilation efficiency for the mixed food (phytoplankton:small detritus=1:1) was measured to be around 0.49. Taking the assimilation efficiency for phytoplankton into account, I calculate that the assimilation efficiency for small detritus is 0.16. This low value agrees with the general understanding that small detritus is a food source of low quality.

Excretion Excretion is formulated as $\varsigma_i Q10^{(T-T_{ref})/10}$ where the term ς_i is the excretion rate, $Q10$ is a measure of the variation in the excretion rate when there is a 10°C temperature rise, and T_{ref} is a reference temperature. The value of ς_i is given following Gaudy et al. (2000). The ammonia excretion rates of *Acartia clausi* copepodite and adult were measured in Gaudy et al. (2000) to be $2.48\pm0.62\times10^{-4}$ μg atom N h^{-1} ind^{-1} at 10°C, salinity 35. Taking the reference individual body weight of copepodite and adult (shown in Table 3.1) into account, the range of the ammonia excretion rate for copepodite is 3.97-4.95% d^{-1}, and for adult is 1.06-1.3% d^{-1}. In the model, I set the excretion rate of copepodite to be 4.0% d^{-1} and the excretion rate of adult to be 1.3% d^{-1}. Since there were no measurements of the excretion rate of nauplius, I set the value of the excretion rate of nauplius to be 4.0% d^{-1} referring to the excretion rates of copepodite and adult. In Gaudy et al. (2000), they also measured the excretion rate at 20°C, salinity 35 to be $5.56\pm1.74\times10^{-4}$ μg atom N h^{-1} ind^{-1}. According to the definition of Q10, I calculate that the value of Q10 for *Acartia clausi* ranges from 1.26 to 3.97. In the model, I set the value of Q10 to be 2.58.

3.2.2.3 Life cycle stage transition

Life cycle stage transition means the biological processes: moulting ($\iota_{2,3}$ and $\iota_{3,4}$) and hatching ($\kappa_{1,2}$).

Moulting Moulting is the consequence of growth. When copepod individuals of early life cycle stage grow to a certain point and reach a threshold body weight, they moult to the next life cycle stage. The parametrization of moulting includes in the model the transfer of biomass (Z_i) and abundance (A_i) from nauplius to copepodite and from copepodite to adult. I use an individual body weight dependent sigmoidal function to calculate the moulting rate:

$$\iota_{i,j} = m_{i,j} f_4(W_i) \quad , \tag{3.6}$$

where $f_4(W_i)$ is

$$f_4(W_i) \;=\; \begin{cases} \frac{(W_i - W_{ref_i})^2}{(W_i - W_{ref_i})^2 + k_{w_i}^2} & \text{when } W_{ref_i} < W_i \\ 0 & \text{when } W_{ref_i} > W_i \end{cases} \quad .$$

In Equation 3.6, the term $m_{i,j}$ is the maximum moulting rate with value of 1 d^{-1}, the term W_{ref_i} is the reference individual body weight, and k_{w_i} is a curve factor. The equation controls that the moulting is inhibited before the individual body weight (W_i) reaches the reference individual body weight (W_{ref_i}), and from the reference individual body weight, the moulting rate increases gradually to 1 d^{-1}.

Hatching The hatching of copepod eggs is controlled by the temperature. With Bělehrdek's empirical function (Bělehrádek, 1935), the hatching time (time needed for hatching) can be estimated (McLaren et al., 1969). General formulation of Bělehrdek's empirical function is $D = a(T - b)^c$, where D is the hatching time of egg (in day), a is a fitting factor (in d $°C^{-1}$), and c is a dimensionless constant. The parameters a and c control the sensitivity of the equation to the variations in the temperature, b is a reference temperature (in °C) referring to 'biological zero' temperature at which the metabolic activity of eggs stops.

The relation between temperature and hatching time is well studied in eggs of *Acartia spp.* (McLaren et al., 1969; McLaren, 1978; Uye, 1980). There are two observations in the North Atlantic about *Acartia clausi* egg development, one is from McLaren et al. (1969) in Nova Scotia ($D = 1163(T + 8.2)^{-2.05}$) and the other is from McLaren (1978) in L. Striven, west coast of Scotland ($D = 1442(T + 10.49)^{-2.05}$). I use the latter empirical equation to parametrize the hatching rate because it is observed in the sea area very close to the North Sea.

Bělehrdek's empirical function expresses the relation between hatching time and temperature. In the model, I need to convert the hatching time-temperature relation into hatching rate-temperature relation. Two steps are conducted for this purpose. Firstly, the hatching time under different temperatures are calculated with the empirical function. Then, the relation between the reciprocal of the hatching time (the hatching rates) and temperatures are fitted with equation:

$$\kappa_{1,2} = m_{1,2}\ \exp(n\ (T - T_{scale})) \quad , \tag{3.7}$$

where the term T is temperature and n is a fitting factor. T_{scale} is a reference temperature. The value of T_{scale} is 20°C. The value of n is decided by fitting the equation 3.7 to reproduce the hatching rate.

3.2.2.4 Mortality

The parametrization of the mortality rate is difficult because the mechanism regulating the mortality rate is poorly understood. There are several reasons that could cause deaths of copepods: disease, starvation and predation by higher trophic levels. In the model, I use a constant mortality rate plus a body weight dependent mortality rate to take these factors into account. The constant mortality rate accounts for disease and predation related death and the body weight dependent mortality rate accounts for starvation related death. Starvation mortality is an important non-predatory source of death (Lynch, 1983). I use a body weight dependent mortality to parametrize this effect because Threlkeld (1976) suggested that the survival time of zooplankton under conditions of starvation could be calculated with the excretion rate and the fraction of initial body weight that could be lost prior to death. According to the Chossat's rule (Kleiber, 1961), in the absence of predators, the mortality rate can be 100% when the body weight is decreased by half due to starvation. In the model, I parametrize the body weight dependent mortality based on this rule. The function used to calculate the mortality rate is

$$\eta_i = (r_{max} - r_i)\ \omega_i\ \exp(-f_{c_i}\ \frac{W_i}{W_{ref_i}}) + r_i \quad , \tag{3.8}$$

where the term r_{max} is the maximum mortality rate with the value as 1 d^{-1}, r_i is the constant mortality rate of different life cycle stages, f_{c_i} is a curve constant, controlling

the shape of the body weight dependent mortality rate, and ω_i is a switch controlling for which life cycle stage the body weight dependent mortality rate is activated.

Acartia clausi is a broadcast spawner, which lays eggs directly into the outside environment. The mortality of its eggs is very high. For this reason, I set the mortality rate of eggs to be 15% d^{-1}. The constant mortality rates of nauplius, copepodite and adult are set to be 0.4% d^{-1}, 0.36% d^{-1} and 0.36% d^{-1}, respectively according to the observed levels in the North Sea in Hay et al. (1988).

3.2.2.5 Parameter values

Depending on the sources of the values, four groups of parameters are discerned. The first group is the parameters with robust values taken from previous literature. These parameters are weights of different life cycle stages and parameters used to parametrize the well investigated biological process, the hatching of egg. The second group is the parameters whose values are derived from results of the laboratory experiments that study particular biological processes of *Acartia clausi*. These parameters are the main part of the model parameters. These parameters include the half saturation coefficient in the food dependent ingestion, the optimum temperature for ingestion, $Q10$, the excretion rates and the constant mortality rates. The third group is the parameters, whose values are derived from the observations that are related to the other *Acartia* species or general information on copepods with reasonable assumptions. These parameters are the maximum ingestion rates and the body weight related mortality rates. The fourth group is the parameters whose values are estimated with the laboratory observation data. They are curve factors in the food dependent ingestion and the reference temperatures in the temperature dependent ingestion.

The values of the reference, maximum and minimum individual body weights are listed in the Table 3.1. The values of the other parameters are summarized in Table 3.2.

Source data (dry weight per individual)								
Citation	Egg	NI	NII	NIII	NIV	NV	NVI	Unit
Hay et al. (1988)	0.1	0.1	0.149	0.212	0.285	0.387	0.517	μg

Parameter values in this study				
Life cycle stage	Egg		Nauplius	
	μg ind^{-1}	mmol N ind^{-1}	μg ind^{-1}	mmol N ind^{-1}
W_{ref}	0.1	5.03e-07	0.275	1.38e-06
W_{min}	-	-	0.1	5.03e-07
W_{max}	-	-	0.51	2.58e-06

Source data (dry weight per individual)								
Citation	C1	C2	C3	C4	C5	Male	Female	Unit
Hay et al. (1988)	0.338	0.703	1.407	2.388	4.305	6.326	7.724	μg

Parameter values in this study				
Life cycle stage	Copepodite		Adult	
	μg ind^{-1}	mmol N ind^{-1}	μg ind^{-1}	mmol N ind^{-1}
W_{ref}	1.83	9.2e-06	7.03	3.5e-05
W_{min}	0.517	2.6e-06	5.31	2.7e-06
W_{max}	4.305	2.2e-05	8.0	4.0e-05

Table 3.1: The reference, minimum and maximum individual body weights for each life cycle stage. The dry weight in unit μg per individual is converted to mmol N per individual by assuming that 40% of the dry weight is carbon and using the gram to mole conversion of carbon and the Redfield ratio (C:N=6.625).

Parameters	Z_1	Z_2	Z_3	Z_4	Unit
Ingestion					
$g_{i_{\max P}}$	-	2.8	1.8	0.58	d^{-1}
$g_{i_{\max D}}$	-	5.6	3.6	1.16	d^{-1}
k_P	-	2.3	2.3	2.3	mmol N m^{-3}
k_{D_s}	-	5.75	5.75	5.75	mmol N m^{-3}
α	-	2.75	2.75	2.75	-
T_{opt}	-	15	15	15	°C
T_1	-	1	1	1	°C
T_2	-	6.5	6.5	6.5	°C
Moulting					
k_{w_i}	-	1.2e-06	1.3e-06	5.0e-06	mmol N ind^{-1}
Hatching					
T_{scale}	20	-	-	-	°C
n	0.1085	-	-	-	$°C^{-1}$
$m_{1,2}$	1	-	-	-	d^{-1}
Egestion and excretion					
β_P	-	0.77	0.77	0.77	-
ς_i	-	4.0%	4%	1.3%	d^{-1}
$Q10$	-	2.58	2.58	2.58	-
T_{ref}	-	10	10	10	°C
Mortality					
f_{c_i}	-	9.5	9.5	9.5	-
r_{max}	100%	100%	100%	100%	d^{-1}
r_i	15%	4.0%	3.6%	3.6%	d^{-1}
ω_i	0	1	1	1	-

Table 3.2: The parameter values in the life cycle model of *Acartia clausi*.

3.3 Model application and results

The life cycle model is coded with the numeric computing language, Matlab (Matrix Laboratory). I use the high order solver (ODE 45) of the ordinary differential equation

to solve the prognostic equations of each life cycle stage.

In order to estimate the values of the curve factor (α) in the food dependent ingestion (Equation 3.3) and the reference temperatures (T_1 and T_2) in the temperature dependent ingestion (Equation 3.4), I simulate the model in constant environmental conditions (temperature and food levels) according to the laboratory experimental setups from Klein Breteler and Schogt (1994). Three groups of simulations are conducted. The first group is at 5°C under the food concentration of 1.4 and 2.6 mmol N m^{-3} (food concentration equals to 111 and 206 μg C l^{-1}, firstly, I use gram to mole conversion of carbon to convert the unit μg C l^{-1} into mmol C l^{-1} and then Redfield ratio C:N=6.625 to convert the unit mmol C l^{-1} into mmol N m^{-3}); the second group is at 10°C, 1.0 and 1.6 mmol N m^{-3} (79 and 127 μg C l^{-1}); the third group is at 15°C, 1.0 and 1.4 mmol N m^{-3} (79 and 111 μg C l^{-1}). Because in the laboratory experiments in Klein Breteler and Schogt (1994), only algae were fed to *Acartia clausi*, in this chapter, I apply only phytoplankton as food source.

In each simulation, the ontogenetic development time of one single cohort (1000 individuals m^{-3}) from egg to adult is simulated. The development time is determined when half of the population reaches the adulthood. The time step of the model is 3600 model seconds. I run all simulations for 200 model days.

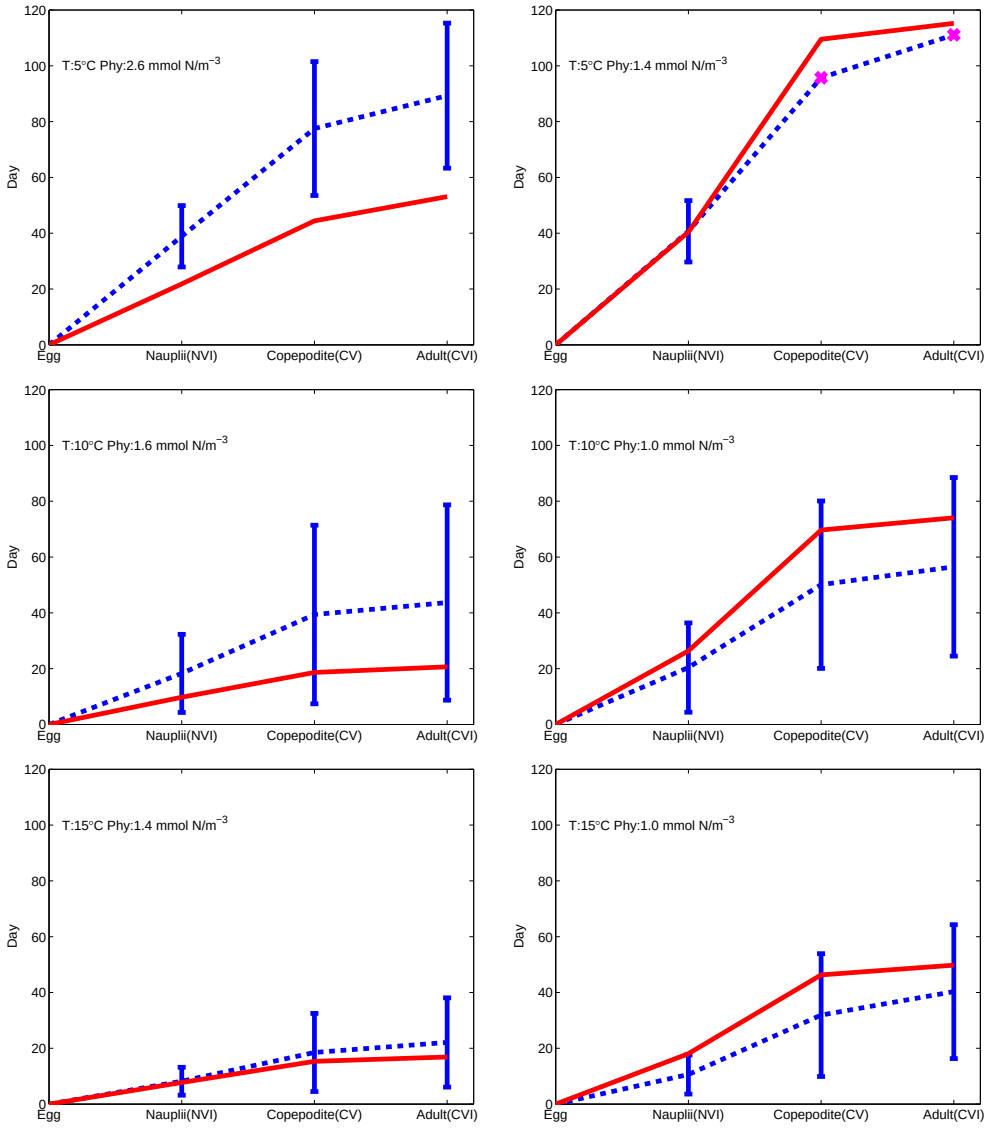

Figure 3.1: The generation development time from the model results (solid red line) and experimental data (dashed blue line). For the observation, the standard deviation of the development time is displayed with blue solid line. The magenta crosses at 5°C, 1.4 mmol N m^{-3} mean missing data. In Klein Breteler and Schogt (1994), at 5°C, 1.4 mmol N m^{-3}, *Acartia clausi* cohort failed to develop to the life cycle stages CVI and CV before died out. When the observation data were not available, Klein Breteler and Schogt (1994) provided estimations with a fitting function.

The model results of each simulation and the experimental data from Klein Breteler and Schogt (1994) are displayed in Figure 3.1. The food dependent ingestion is tested at the same temperatures with different food concentrations. At 5°C, the difference of the development time between model result and experimental data is less than 5 days under the lower food concentration (1.4 mmol N m^{-3}) but at the higher

food concentration (2.6 mmol N m^{-3}), the model result is not in a reasonable range compared with the experimental data. At 10 and 15°C, the model results are in a reasonable range compared with the experimental data under both higher food concentrations (10°C, 1.6 mmol N m^{-3}; 15°C, 1.4 mmol N m^{-3}) and lower food concentrations (10°C, 1.0 mmol N m^{-3}; 15°C, 1.0 mmol N m^{-3}). This means that the parametrized food dependent ingestion in the model has better performance at 10 and 15°C than at 5°C. The food dependent ingestion is parametrized with Equation 3.3, in which the half saturation coefficient is the key parameter. The value of the half saturation coefficient is 2.3 mmol N m^{-3}. This value is given according to the observation in Mayzaud et al. (1998). They did the laboratory experiments at 14-15°C. It appears that the observed value of the half saturation coefficient is overestimated when applied to 5°C. This may lead to an underestimation of the development time, especially when the model is applied to simulate the development time in the conditions with low temperatures and high food concentrations.

In this thesis, I intend to model the life cycle dynamics of *Acartia clausi* in the North Sea. The annual range of SST in the open North Sea is 5-16°C (Janssen et al., 1999; Becker and Schulz, 2000) and the food concentrations exhibiting as surface chlorophyll concentrations ranges from 1 to 4 mg chl m^{-3} (equals to 0.62-2.48 mmol N m^{-3} when assuming that 1 mg Chl=50 mg C (Radach and Pätsch, 1997) and using the gram to mole conversion of carbon and the Redfield ratio to convert the unit mg C to mmol N) in the central and northern North Sea (Radach and Pätsch, 1997). When SST is low, e.g. in winter, the food concentration is also low. The experimental setup of low temperature, high food concentration (5°C, 2.6 mmol N m^{-3}) is rare in reality. Since the value of the half saturation coefficient adopted from Mayzaud et al. (1998) is sufficient in representing the experimental data at 10 and 15°C and the measurement of the value of the half saturation coefficient at low temperatures is rare in previous literature, I keep the value from Mayzaud et al. (1998). In order to reduce the difference between the development time under higher and lower food concentrations at low temperatures, I set the value of α to be 2.75.

The values of T_1 and T_2 in the temperature dependent ingestion are estimated by comparing the model results to the experimental data in the conditions with similar food concentrations and different temperatures. The experimental data show that when the temperature increases from 5 to 10°C (from 5°C, 1.4 mmol N m^{-3} to 10°C,

1.6 mmol N m^{-3}), the development time is decreased by 69 days and when temperature rises from 10 to 15°C (10°C, 1.0 mmol N m^{-3}; 15°C, 1.0 mmol N m^{-3}), the development time is decreased by 20 days. This implies that under similar food concentrations, the development time decreases with rising temperature. I choose the values for T_1 and T_2 to be 1 and 6.5°C, which can reproduce the experimental data.

3.4 Sensitivity experiments

In this section, I study the sensitivity of the development of *Acartia clausi* to variations in the temperature and food concentration at different temperature conditions with sensitivity experiments. The sensitivity experiments are conducted based on two scenarios: 6°C, 1.4 mmol N m^{-3} (REF1) and 12°C, 1.4 mmol N m^{-3} (REF2). I choose the temperatures to be 6°C and 12°C because at the Stonehaven sampling station, in March the monthly mean SST is around 6°C and in August/September the monthly mean SST is 12-14°C. Two group of sensitivity experiments are conducted. The first group is to increase or decrease the temperature by 1°C: STI1 (Sensitivity experiment: the Temperature is Increased in scenario 1), STD1 (Sensitivity experiment: the Temperature is Decreased in scenario 1), STI2 and STD2. The second group is to increase or decrease the food concentration by 10%: SFI1 (Sensitivity experiment: the Food concentration is Increased in scenario 1), SFD1 (Sensitivity experiment: the Food concentration is Decreased in scenario 1), SFI2 and SFD2. In each sensitivity experiment, the development time is calculated. In the following table, I give a summary of the simulations conducted in this section.

	Simulation	Condition
Reference scenarios	REF1	6°C, 1.4 mmol N m^{-3}
	REF2	12°C, 1.4 mmol N m^{-3}
Temperature±1°C	STI1	7°C, 1.4 mmol N m^{-3}
	STD1	5°C, 1.4 mmol N m^{-3}
	STI2	13°C, 1.4 mmol N m^{-3}
	STD2	11°C, 1.4 mmol N m^{-3}
Food concentration±10%	SFI1	6°C, 1.54 mmol N m^{-3}
	SFD1	6°C, 1.26 mmol N m^{-3}
	SFI2	12°C, 1.54 mmol N m^{-3}
	SFD2	12°C, 1.26 mmol N m^{-3}

Table 3.3: An overview of the setups of the sensitivity experiments in Section 3.4.

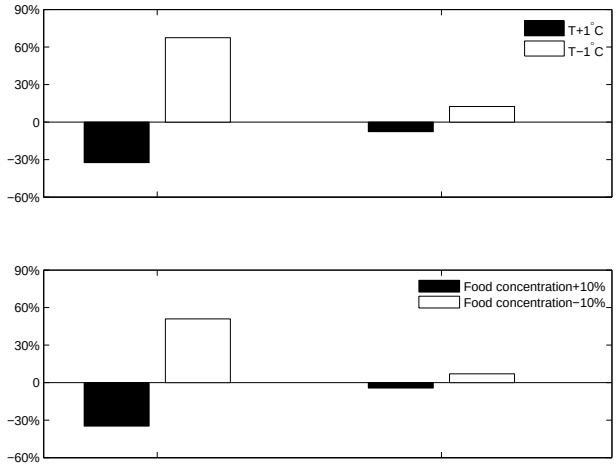

Figure 3.2: Percentage changes of the development time when a decrease (dark bar) or an increase (light bar) are made to the temperature and food concentration. In the upper panel, the temperatures in REF1 and REF2 are increased or decreased by 1°C, from left to right, the bars mean (STI1-REF1)/REF1, (STD1-REF1)/REF1, (STI2-REF2)/REF2 and (STD2-REF2)/REF2; in the lower panel, the food concentration in REF1 and REF2 are increased or decreased by 10%, from left to right, the bars means (SFI1-REF1)/REF1, (SFD1-REF1)/REF1, (SFI2-REF2)/REF2 and (SFD2-REF2)/REF2.

The results of the sensitivity experiments are shown in Figure 3.2. The results show that under the same food concentration, the percentage changes of the development time induced by temperature changes are higher at 6°C than that at 12°C.

At different temperatures, the percentage changes of the development time induced by changes in food concentrations are also higher at 6°C than at 12°C. The results suggest that the development of *Acartia clausi* is much more sensitive to variations in the temperature and food concentration at low temperature conditions than at high temperature conditions.

3.5 Summary and discussion

In this chapter, I develop a life cycle model for *Acartia clausi* to study the sensitivity of the development of *Acartia clausi* to variations in the temperature and food concentration at different temperature conditions. The life cycle model is developed using a similar model structure as in Fennel (2001). The biological processes of *Acartia clausi* are parametrized according to the information published in literature.

The model is applied to simulate the development time from egg to adult in different environmental conditions and the model results are compared to the experimental data from Klein Breteler and Schogt (1994). The model results show that the model is able to reproduce the experimental data at 10 and 15°C under both the high and low food concentrations. At 5°C, the model is able to reproduce the observed development time under the low food concentration but under the high food concentration, the model result is not in a reasonable range compared to observations. The reason for this discrepancy is that the current value for the half saturation coefficient in the food dependent ingestion, which is taken from Mayzaud et al. (1998), was measured at 14-15°C. When applied this value to model the development time in the condition with low temperature and high food concentration, the development time may be underestimated. More measurements of the ingestion of *Acartia clausi* at low temperature are needed in order to improve the model performance.

The results of the sensitivity experiments show that the development of *Acartia clausi* is more sensitive to variations in the temperature and food concentration at low temperature conditions than at high temperature conditions. This model result can be used to better understand the observed mismatch between the seasonal variations of the chlorophyll concentration and *Acartia clausi* abundance at the Stonehaven sampling station. The earliest timing of the annual maximum surface chlorophyll concentration

peak observed at the Stonehaven sampling station during the observation period is in week 15. But before week 21 it is unlikely that the *Acartia clausi* copepodite abundance can reach 10% of the abundance of its annual maximum peak (chance is less than 0.5%). The main reason for this mismatch is that the low temperature (5-7°C) during the spring phytoplankton bloom suppresses the development of *Acartia clausi*. This phenomena was also reported in Colebrook (1982), in which the long time series continuous plankton record data from the North Atlantic and the North Sea were analyzed. The mismatch induced by the low temperature at the beginning of the growing season is severely affecting the energy transfer from phytoplankton to zooplankton. Only less than 10% of the phytoplankton production in spring and early summer are directly utilized by zooplankton (Fransz and Gieskes, 1984; Smetacek, 1984). The results of the sensitivity experiments imply that future climate warming will benefit *Acartia clausi*. Due to climate warming, the temperature at the beginning of growing season will be increased and the timing of the phytoplankton bloom will be earlier (earlier timing of the phytoplankton bloom due to climate variations in the North Sea has already been reported, e.g., in Edwards and Richardson (2004)). Both of the two effects will accelerate the development of *Acartia clausi* at the beginning of the growing season. Thus, in the future a better match between phytoplankton and *Acartia clausi* at the beginning of growing season is expected.

Chapter 4

Modelling the seasonal variation of *Acartia clausi* abundance under different reproductive patterns

4.1 Introduction

Resting stage formation as a mechanism to overcome adverse environmental conditions is a well-known life history strategy. Copepods are an important group of zooplankton in oceans, and so far more than 50 species of marine copepods have been reported to produce resting eggs (e.g., Uye, 1985; Dahms, 1995; Marcus, 1996; Engel and Hirche, 2004). The production of resting eggs is often performed to overcome harsh environmental conditions. The fluctuation in temperature is reported to be the main factor inducing the production of resting eggs (Grice and Marcus, 1981; Uye, 1985; Sullivan and McManus, 1986).

Acartia clausi has been reported to produce resting eggs. In Akkeshi Bay (northeast of Japan), where the water temperature dropped to -2°C in winter, resting eggs from *Acartia clausi* were found in abundance of 10^4-10^5 m^{-2} on the seafloor in November and February (Uye, 1985). Also, *Acartia clausi* was found to lay resting eggs that stay unhatched for about two weeks when in summer the temperature reached above 22°C in the Inland Sea of Japan (Uye, 1985). *Acartia clausi* produced resting eggs

to overcome the time period of high sea temperature. Resting eggs of this species for similar purposes were also reported by Sullivan and McManus (1986).

In the North Sea, resting eggs belonging to *Acartia spp.* were found in winter near the English Channel (Lindley, 1990) and Helgoland (Engel and Hirche, 2004). These observations implied that *Acartia clausi* might produce resting eggs in the North Sea, although the researchers did not taxonomically determine to which *Acartia* species these resting eggs belonged. According to Uye (1985), *Acartia clausi* produces resting eggs may be for two purposes. One is for overwintering and the other is for overcoming the hot summer. In the North Sea, the water temperature in summer rises rarely above 20°C, it is unlikely that *Acartia clausi* needs to produce resting eggs to overcome the hot summer time as in the Inland Sea of Japan. If resting eggs are produced by this species in the North Sea, they may be used as an overwintering strategy.

Whether the production of resting eggs should be included in the life cycle model of *Acartia clausi* becomes an important question. Firstly, reproductive pattern directly determines the seasonal variation of *Acartia clausi* abundance. Secondly, resting eggs may be used as an overwintering strategy. The composition and abundance of the overwintering stocks are important factors determining the seasonal variation of copepod abundance. In this chapter, I will model the seasonal variations of *Acartia clausi* abundance considering different reproductive patterns and compare the model results to the seasonal variation of *Acartia clausi* abundance at the Stonehaven sampling station. This allows to address the question whether it is necessary to include resting egg production into the life cycle model as an overwintering strategy.

Three types of eggs, that differ in their modes of the development, have been distinguished: subitaneous eggs, dormant eggs (diapause eggs) and quiescent eggs. Quiescent eggs are very similar to subitaneous eggs. Subitaneous eggs hatch in a few days after being produced, regardless of variations in the environmental conditions. The hatching of quiescent eggs is related to environmental conditions. Generally, they hatch soon after being produced but they are also able to delay their hatching in response to deteriorating environmental conditions, e.g. changes in the temperature or oxygen concentration. Dormant eggs are very different from quiescent eggs and subitaneous eggs because the hatching of dormant eggs is not possible before they have completed a refractory phase (dormancy period) (Grice and Marcus, 1981). The length

of the dormancy period varies for different species, lasting from a few weeks to several months or even to several years.

The reproductive patterns in this chapter are different in the types of eggs produced. If assuming that *Acartia clausi* in the North Sea produces resting eggs for overwintering, in principal there are three possibilities for the reproductive pattern. The first one is a combination of subitaneous eggs and quiescent eggs, the second one is subitaneous eggs and dormant eggs, and the third one is subitaneous eggs, dormant eggs and quiescent eggs all together. Since subitaneous eggs and quiescent eggs are very similar and in Chapter 3, I have already introduced a temperature dependent hatching trigger that is able to delay the hatching of subitaneous eggs in low temperatures, in this chapter I treat both egg types in the same way (this egg type is called the subitaneous egg). For simplicity, two reproductive pattern are considered in the model: subitaneous eggs only or a combination of subitaneous eggs and dormant eggs.

4.2 Model description

In Chapter 3, I model the development of *Acartia clausi* from egg to adult in different environmental conditions. In this chapter, I focus on the seasonal variation of *Acartia clausi* abundance in the North Sea, the life cycle model of *Acartia clausi* is thus needed to include the parametrizations of reproduction and other biological processes related to different types of eggs, such as dormancy period and the hatching of dormant eggs. In the following sections, I will introduce the parametrizations of these biological processes, and a Phytoplankton-Nutrient-Detritus (PND) model to which *Acartia clausi* life cycle model is coupled.

4.2.1 *Acartia clausi* life cycle model

4.2.1.1 Equation system

Since the resting egg production is taken into consideration, there are then six life cycle stages in the present life cycle model of *Acartia clausi*: subitaneous egg, nauplius (NI-NVI), copepodite (CI-CV), adult, and two dormant egg stages: immature

dormant egg and mature dormant egg (for convenience, I label them as i=1, 2, 3, 4, 5, 6, respectively). For each life cycle stage the biomass $\left[\vec{Z} = (Z_1, Z_2, Z_3, Z_4, Z_5, Z_6)\right]$ (mmol N m^{-3}) and the abundance $\left[\vec{A} = (A_1, A_2, A_3, A_4, A_5, A_6)\right]$ (individuals m^{-3}) are resolved. The ordinary differential equations are:

$$\begin{aligned} \frac{d\vec{Z}}{dt} &= \mathbf{M_Z}\vec{Z}' \\ \frac{d\vec{A}}{dt} &= \mathbf{M_A}\vec{A}' \quad , \end{aligned} \tag{4.1}$$

where the non-linear matrices (M_Z and M_A) are:

$$\mathbf{M_Z} = \begin{pmatrix} \psi_1 - \tau_{1,2} & 0 & 0 & +\tau_{4,1} & 0 & 0 \\ +\tau_{1,2} & \psi_2 - \tau_{2,3} & 0 & 0 & 0 & +\tau_{6,2} \\ 0 & +\tau_{2,3} & \psi_3 - \tau_{3,4} & 0 & 0 & 0 \\ 0 & 0 & +\tau_{3,4} & \psi_4 - \tau_{4,1} - \tau_{4,5} & 0 & 0 \\ 0 & 0 & 0 & +\tau_{4,5} & \psi_5 - \tau_{5,6} & 0 \\ 0 & 0 & 0 & 0 & +\tau_{5,6} & \psi_6 - \tau_{6,2} \end{pmatrix} ,$$

$$\mathbf{M_A} = \begin{pmatrix} \phi_1 - \tau_{1,2} & 0 & 0 & +\tau_{4,1} & 0 & 0 \\ +\tau_{1,2} & \phi_2 - \tau_{2,3} & 0 & 0 & 0 & +\tau_{6,2} \\ 0 & +\tau_{2,3} & \phi_3 - \tau_{3,4} & 0 & 0 & 0 \\ 0 & 0 & +\tau_{3,4} & \phi_4 - \tau_{4,1} - \tau_{4,5} & 0 & 0 \\ 0 & 0 & 0 & +\tau_{4,5} & \phi_5 - \tau_{5,6} & 0 \\ 0 & 0 & 0 & 0 & +\tau_{5,6} & \phi_6 - \tau_{6,2} \end{pmatrix} .$$

In the non-linear matrices, the term $\psi_i = (g_{i_P} + g_{i_{D_s}}) - l_i - \eta_i$ represents the source terms or loss terms of the biomass: ingestion ($g_{i_P}, g_{i_{D_s}}$ when $i = 2, 3, 4$), egestion and excretion (l_i when $i = 2, 3, 4$), and mortality (η_i when $i = 1, 2, 3, 4, 5, 6$); the term $\phi_i = -\eta_i$ represents mortality (η_i when $i = 1, 2, 3, 4, 5, 6$), which is the loss term of the abundance. In the non-linear matrices, the life cycle stage transition rate ($\tau_{i,j}$) represent reproduction ($\lambda_{4,1}$, $\lambda_{4,5}$), hatching ($\iota_{1,2}$, $\iota_{6,2}$), moulting ($\kappa_{2,3}$ or $\kappa_{3,4}$) or immature dormant egg to mature dormant egg transition ($\varpi_{5,6}$). The parametrizations of ingestion, egestion and excretion, moulting, hatching and mortality have already been introduced in Chapter 3 and will not be presented here again.

4.2.1.2 Life cycle stage transition

The parametrizations of reproduction ($\lambda_{4,1}$ or $\lambda_{4,5}$), immature dormant egg to mature dormant egg transfer ($\varpi_{5,6}$) and hatching of mature dormant egg ($\kappa_{6,2}$) are introduced in this section.

Reproduction Reproduction of adults only happens when the individual body weight of adult exceeds the reference individual body weight of adult. A part of biomass from female adults is provided to produce eggs. The reproduction rate $\lambda_{4,j}$ ($j = 1, 5$) is calculated with the equation:

$$\lambda_{4,j} = \delta \rho_{fem} f_4(W_4) \varepsilon_j \quad , \tag{4.2}$$

where the term δ is the maximum reproduction rate, ρ_{fem} is the proportion of females. The limitation function $f_4(W_4)$ is calculated as

$$f_4(W_4) = \begin{cases} \frac{(W_4 - W_{ref_4})^2}{(W_4 - W_{ref_4})^2 + k_{w_4}^2} & \text{when } W_{ref_4} < W_4 \\ 0 & \text{when } W_{ref_4} > W_4 \end{cases} ,$$

where the term W_4 is the individual body weight of adult, which is calculated as the ratio of the total adult biomass to total adult abundance, the term W_{ref_4} is the reference individual body weight of adult and the term k_{w_4} is a curve factor. The term ε_j is the proportion of subitaneous egg or immature dormant egg to the total egg production as

$$\varepsilon_j = \left\{ \begin{array}{ll} \varepsilon_1 & \text{for subitaneous egg production} \\ \varepsilon_5 & \text{for immature dormant egg production} \\ \varepsilon_1 + \varepsilon_5 = 100\% & \end{array} \right\} .$$

The value of δ is given following Tiselius (1989). Tiselius (1989) observed that the reproduction rate of *Acartia clausi* ranged from 9.7 to 17.5 eggs female^{-1} d^{-1} in the transition zone between the North Sea and the Baltic Sea in July and August. I use the larger value for the maximum reproduction rate in this model. The value of ε_j is set in the sensitivity experiments. I will introduce this later.

Immature dormant eggs to mature dormant eggs transition According to the observation, dormant eggs have to overcome a dormant period before the hatching is possible. Following the model design from Hense and Beckmann (2010), I parametrize

a dormancy period for the immature dormant eggs in the model. The dormancy period is calculated with the following equation:

$$\chi_{dorm} = \frac{1}{Z_{5_{max}}(t_o, t)} \int_{t_o}^{t} Z_{5_{max}}(t_o, t')\ dt' \quad , \tag{4.3}$$

where the expression

$$Z_{5_{max}}(t_o, t) = \max(\{Z_5\}_{t_o}^{t})$$

is the maximum immature dormant egg biomass during the time period (from t_o to t). With this equation, the dormancy period is counted from the time (t_o) when the female adults begin to produce immature dormant eggs. When the required dormancy period (D_{th}) is reached, the immature dormant eggs are transferred to mature dormant eggs.

Hatching of subitaneous eggs and mature dormant eggs The hatching of the mature dormant egg ($\kappa_{6,2}$) and the subitaneous egg ($\kappa_{1,2}$) are parametrized with equations:

$$\begin{aligned} \kappa_{1,2} &= m_{1,2}\ e^{(n\ (T-T_{scale}))} \\ \kappa_{6,2} &= m_{6,2}\ e^{(n\ (T-T_{scale}))} \quad , \end{aligned} \tag{4.4}$$

where the terms $m_{1,2}$ and $m_{6,2}$ are the maximum hatching rate with value 1 d^{-1}, the terms n and T_{scale} and their values have already been introduced in Section 3.2.2.3.

4.2.1.3 Parameter values in the life cycle model of *Acartia clausi*

The parameter values are listed in Table 4.1. The sources of most parameter values listed have been introduced in Chapter 3. In this chapter, I include immature dormant eggs and mature dormant eggs into the life cycle model of *Acartia clausi*. There are no measurements of the length of the dormancy period of dormant eggs from *Acartia clausi*. In the model, I assume that the length of the dormancy period (D_{th}) to be 270 days, making sure that the dormant eggs hatch after winter (after February). This assumption is made based on the concept that copepods produce dormant eggs to overcome harsh environmental conditions. The mortality rates of immature dormant eggs and mature dormant eggs are given according to Sichlau et al. (2011). They measured the mortality rate of dormant eggs from *Acartia spp.* near the island Fünen,

Denmark to be 35%-53% year^{-1}. In the model, I set the mortality rate of dormant eggs according to the higher measured value. The individual body weights of immature dormant eggs and mature dormant eggs are set to be the same as the individual body weight of subitaneous eggs.

Parameters	Z_1	Z_2	Z_3	Z_4	Z_5	Z_6	Unit
Ingestion							
$g_{i_{\max_D}}$	-	5.6	3.6	1.16	-	-	d^{-1}
$g_{i_{\max_P}}$	-	2.8	1.8	0.58	-	-	d^{-1}
k_{D_s}	-	5.0	5.0	5.0	-	-	mmol N m^{-3}
k_P	-	2.0	2.0	2.0	-	-	mmol N m^{-3}
T_{opt}	-	15	15	15	-	-	°C
T_1	-	1	1	1	-	-	°C
T_2	-	7	7	7	-	-	°C
α	-	3.5	3.5	3.5	-	-	-
Moulting							
k_{w_i}	-	1.2e-06	1.3e-06	-	-	-	mmol N ind^{-1}
Reproduction							
k_{w_4}	-	-	-	5.0e-06	-	-	mmol N ind^{-1}
δ	-	-	-	0.25	-	-	d^{-1}
ρ_{fem}	-	-	-	80%	-	-	-
ε_j*	-	-	-	-	-	-	-
Hatching and immature dormant egg to mature dormant egg transfer							
D_{th}	-	-	-	-	270	-	d
$m_{5,6}$	-	-	-	-	1	-	d^{-1}
$m_{1,2}$	1	-	-	-	-	-	d^{-1}
$m_{6,2}$	-	-	-	-	-	1	d^{-1}
T_{scale}	20	-	-	-	-	20	°C
n	0.1085	-	-	-	-	0.1085	°C^{-1}
Egestion and metabolism							
β_P	-	0.77	0.77	0.77	-	-	-
β_{D_s}	-	0.16	0.16	0.16	-	-	-
ς_i	-	10.5%	5.5%	4.4%	-	-	d^{-1}

Continued on next page

Table 4.1 – Continued from previous page

Parameters	Z_1	Z_2	Z_3	Z_4	Z_5	Z_6	Unit
$Q10$	-	2.58	2.58	2.58	-	-	-
T_{ref}	-	10	10	10	-	-	°C
Mortality							
f_{c_i}	-	9.5	9.5	9.5	-	-	-
r_{max}	-	100%	100%	100%	-	-	d^{-1}
r_i	15%	3%	1.5%	1.5%	0.6%	0.6%	d^{-1}
ω_i	0	1	1	1	0	0	-
Vertical velocity (assuming upward velocity as positive)*							
w_{Z_i}	-20	0.5	1	1.5	-20	-20	m d^{-1}

Table 4.1: Parameter values in the life cycle model of *Acartia clausi* in Chapter 4. *: the value of ε_j will be set in Section 4.3. *: The description of the vertical velocity is given in Section 4.2.2

4.2.2 PNZD model

Equation system of PNZD model The life cycle model of *Acartia clausi* is coupled to a nitrogen based Phytoplankton-Nutrient-Detritus (PND) model in order to form a complete nutrient cycle. I replace the bulk zooplankton compartment (Z) in the PNZD model from Kühn and Radach (1997) with the life cycle model of *Acartia clausi*. I then couple the PNZD model to a 1-dimensional water column model. The nitrogen fluxes between phytoplankton (P), nutrients (N_u), large detritus (D_l), small detritus (D_s) and zooplankton (Z_i) in the 1-dimensional water column model are described with

equations:

$$
\begin{aligned}
\frac{\partial P}{\partial t} &= \underbrace{\mu_P P}_{\text{phytoplankton growth}} - \underbrace{\sum_{i=2}^{4} g_{i_P} Z_i}_{\text{grazing}} - \underbrace{\eta_P P}_{\text{mortality}} - \underbrace{l_P P}_{\text{exudation}} \\
&\quad - \underbrace{\frac{\partial}{\partial z}(w_P P - A_v \frac{\partial}{\partial z} P)}_{\text{vertical motion and vertical diffusion}} \\
\frac{\partial N_u}{\partial t} &= \underbrace{l_P P}_{\text{exudation}} + \underbrace{\sum_{i=2}^{4} l_i Z_i}_{\text{excretion}} + \underbrace{\gamma(D_l + D_s)}_{\text{remineralization}} \\
&\quad - \underbrace{\mu_P P}_{\text{phytoplankton growth}} - \underbrace{\frac{\partial}{\partial z}(-A_v \frac{\partial}{\partial z} N_u)}_{\text{vertical diffusion}} \\
\frac{\partial Z_i}{\partial t} &= \underbrace{(\beta_{i_P} g_{i_P} + \beta_{i_{D_s}} g_{i_{D_s}}) Z_i}_{\text{net ingestion (i=2-4)}} - \underbrace{l_i Z_i}_{\text{excretion (i=2-4)}} - \underbrace{\eta_i Z_i}_{\text{mortality (i=1-6)}} \qquad (4.5) \\
&\quad - \underbrace{\frac{\partial}{\partial z}(w_{Z_i} Z_i - A_v \frac{\partial}{\partial z} Z_i)}_{\text{vertical motion and vertical diffusion}} \\
\frac{\partial D_l}{\partial t} &= \underbrace{(1-\varphi)(\eta_P P + \sum_{i=1}^{6} \eta_i Z_i)}_{\text{mortality (i=1-6)}} - \underbrace{\gamma D_l}_{\text{remineralization}} \\
&\quad + \underbrace{(1-\varphi)(\sum_{i=2}^{4}((1-\beta_{i_P}) g_{i_P} Z_i + (1-\beta_{i_{D_s}}) g_{i_{D_s}} Z_i))}_{\text{egestion (i=2-4)}} \\
&\quad - \underbrace{\frac{\partial}{\partial z}(w_{D_l} D_l - A_v \frac{\partial}{\partial z} D_l)}_{\text{vertical motion and vertical diffusion}} \\
\frac{\partial D_s}{\partial t} &= \underbrace{\varphi(\eta_P P + \sum_{i=1}^{6} \eta_i Z_i)}_{\text{mortality (i=1-6)}} - \underbrace{\gamma D_s}_{\text{remineralization}} - \underbrace{\sum_{i=2}^{4} g_{i_{D_s}} Z_i}_{\text{ingestion (i=2-4)}} \\
&\quad + \underbrace{\varphi(\sum_{i=2}^{4}((1-\beta_{i_P}) g_{i_P} Z_i + (1-\beta_{i_{D_s}}) g_{i_{D_s}} Z_i))}_{\text{egestion (i=2-4)}} \\
&\quad - \underbrace{\frac{\partial}{\partial z}(w_{D_s} D_s - A_v \frac{\partial}{\partial z} D_s)}_{\text{vertical motion and vertical diffusion}} \quad ,
\end{aligned}
$$

where the terms μ_P, η_P and l_P are respectively the growth rate, mortality rate and exudation rate of phytoplankton, the term γ is the remineralization rate of detritus and the term φ represents the proportion of the small detritus to total detritus. The terms β_{i_P} and $\beta_{i_{D_s}}$ are the assimilation efficiencies of *Acartia clausi* for phytoplankton and small detritus. The terms w_P, w_{N_u}, w_{Z_i}, w_{D_l} and w_{D_s} are vertical velocities of respective ecosystem compartment, the values of which are given at the beginning of the simulation. The term A_v is the vertical diffusivity, the value of which is provided by the 1-dimensional water column model during the simulation.

Growth of phytoplankton Phytoplankton are the primary producers in the food-web. In this thesis, I model the phytoplankton biomass concentration with one bulk model compartment and do not consider the life cycle of different algae species. The growth rate (μ_P) of phytoplankton is limited by light (photosynthetically available radiation, I_{par}) and nutrient (N_u). The phytoplankton growth rate is calculated with the equation:

$$\mu_P = \mu_{P_{max}} \frac{I_{par}}{max(I_0/4, I_{min})} \exp\left(1 - \frac{I_{par}}{max(I_0/4, I_{min})}\right) \frac{N_u}{k_{N_u} + N_u} \quad , \tag{4.6}$$

where the term $\mu_{P_{max}}$ is the maximum phytoplankton growth rate, the terms I_0 and I_{min} are the intensities of the sea surface solar radiation and minimum photosynthetically active solar radiation. The term k_{N_u} is the half saturation nutrient constant, which denotes the slope in the phytoplankton nutrient uptake.

The absorption effect of water and the bioturbidity effect of the organic matters on the incoming solar shortwave irradiance are taken into account when calculating the I_{par} for each depth level. The equation used to calculate I_{par} at water depth (z) is:

$$I_{par}(z) = I_0 \; r_{par} \; [exp(-k_w \; z) + B(z)] \quad , \tag{4.7}$$

where the term r_{par} is the proportion of the solar shortwave irradiance that can be used for the photosynthesis, k_w is the absorption coefficient of water and $B(z)$ denotes the bioturbidity effect of the organic matters. $B(z)$ is calculated with the equation:

$$B(z) = exp[-k_c \int_0^z c(z') \; dz'] \quad , \tag{4.8}$$

where the term k_c is the absorption coefficient of the organic matters and $\int_0^z c(z')\,dz'$ denotes the integral of the organic matter ($c(z')$ is the sum of the biomass concentration of phytoplankton, zooplankton and detritus at specific water level) from surface to depth z. Equation 4.8 calculates the absorption effect of the solar shortwave irradiance by the organic matters from sea surface to depth z.

Parameter values of PND model part The parameter values about the PND model part are listed in the Table 4.2.

Parameters	value	unit
$\mu_{P_{max}}$	2.0	d^{-1}
r_{par}	0.35	-
k_w	0.05	m^{-1}
k_c	0.06	m^2 mmol N^{-1}
I_{min}	35	W m^{-2}
k_{N_u}	1.2	mmol N m^{-3}
η_P	0.02; 0.05*	d^{-1}
γ	0.013	d^{-1}
l_P	0.01	d^{-1}
w_{D_l}	-5	m d^{-1}
w_{D_s}	-0.3	m d^{-1}
w_P	-1	m d^{-1}
φ	30%	-

Table 4.2: The parameter values in the PND model part. *: The mortality rate of phytoplankton in euphotic zone is smaller than that below the euphotic zone (euphotic zone is defined as the water depth (z) where $I_{par}(z)$ has decreased to one fourth of $I_{par}(0)$).

4.3 Model setups and application

I use the one-dimensional water column model, General Ocean Turbulence Model (GOTM) (Umlauf et al., 2005) as the framework for the hydrodynamics of the North Sea and for the coupling of biology and physics. Three scenarios are set up in the North Sea (Figure 4.1) referring to the three subregions that are introduced in section 1.2. The first scenario is located in the northern North Sea where the North Atlantic water mass dominates. The second scenario is in the central North Sea, where the North Atlantic water mass and the continental coastal water mass mix and form the central North Sea water mass. The third one is in the southern North Sea, near the English

Channel. The vertical resolution of the three scenarios is one meter per level. The time step is one model hour.

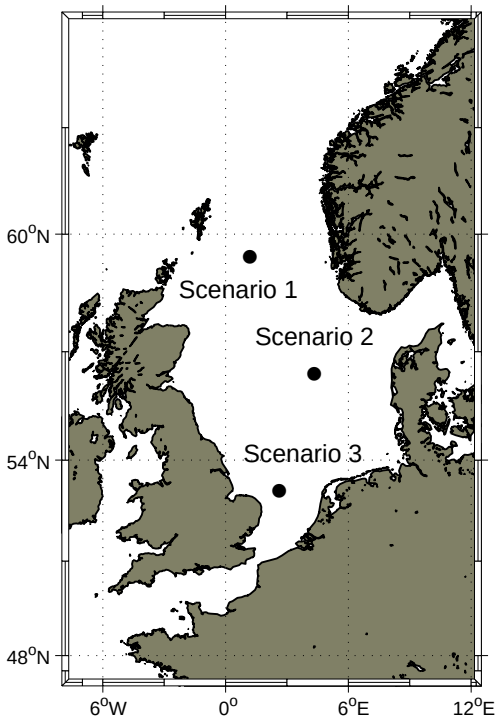

Figure 4.1: From the north to south, three scenarios are set up in the North Sea. The water depths in Scenario 1 (59.1°N, 1.7°E), Scenario 2 (57.3°N, 4.2°E) and Scenario 3 (53.0°N, 2.2°E) are 120 m, 70 m, 40 m, respectively.

Physical model setup The physical model is initialized with temperature and salinity vertical profiles. The wind speed at 10 m height above the sea surface and the sea surface slope gradient in zonal and meridional directions are applied as forcing. The air temperature and relative humidity at 2 m height above the sea surface together with surface air pressure are applied to calculate the sea surface momentum and heat flux with the formular from Kondo (1975). I use the second order model as the turbulence closure. The turbulent kinetic energy and the dissipative length scale are calculated in k-epsilon style. The type of the stability function is set referring to Schumann and Gerz (1995). The values of the coefficients in the second order model are set referring to Cheng et al. (2002), and the parameter values in the k-epsilon model are given according to Rodi (1987).

The data used to set up the physical model of the three scenarios are from different sources. The salinity and temperature profiles are from a high resolution 3D

North Sea circulation model (HAMSOM) (Chen et al., 2012). Based on the salinity and temperature data from Chen et al. (2012), that are daily mean values from 1970-2001, I generate a climatological daily mean temperature and salinity time series data for one year. The climatological data such as the wind speed, relative humidity, cloud coverage and air temperature are from NCEP/NCAR reanalysis 1 (Kalnay et al., 1996) daily mean data. I take the daily mean meteorological data from 1970-2001 and generate a climatological daily mean time series data for one year. In order to produce a meteorological forcing with the temporal resolution as 6 hours, I interpolate linearly between the climatological daily mean values. The surface air pressure in the model are assumed to be constant as 101.3 kPa. The surface slope gradient data are taken from the GOTM scenario 'Annual North Sea Simulation' (Burchard, 1999; Bolding et al., 2002), which are generated from observations during autumn 1998 based on the harmonic analysis of four partial tides. The internal pressure gradients are set to zero. I repeat the forcing every model year.

Biological model setup For the biological model, I choose the second-order modified Patankar-Runge-Kutta scheme as the ordinary differential equation solver. This solver ensures that the values of biological compartments are positive and the total biomass in the ecosystem model is conservative. The vertical resolution and time step of the biological model are set to be the same as in the physical model.

For each of the three locations, two model simulations with different reproductive patterns are carried out: only subitaneous eggs are produced ($\varepsilon_1 = 100\%$ and $\varepsilon_5 = 0\%$) and subitaneous eggs, and dormant eggs are simultaneously produced ($\varepsilon_1 = 70\%$ and $\varepsilon_5 = 30\%$). For convenience, I label them as SE1,2,3 (only Subitaneous Egg) and DS1,2,3 (both Dormant egg and Subitaneous egg). The values of ε_1 and ε_5 in DS1,2,3 are set referring to the observation from Uye (1985) that the ratio of subitaneous eggs to dormant eggs produced by *Acartia clausi* in the Inland Sea of Japan in June was close to 7:3. Since the factors inducing the production of dormant eggs in *Acartia clausi* have not been fully understood yet, it is hard to quantify when and under which conditions dormant eggs are produced. Therefore, I assume that dormant eggs are produced simultaneously with subitaneous eggs.

The initial conditions of the biological model in every sensitivity experiment are listed in the Table 4.3.

Parameter	value	unit
P	0	mmol N m^{-3}
N_u	4.5	mmol N m^{-3}
D_l	4.5	mmol N m^{-3}
D_s	0	mmol N m^{-3}
A_1	10000	individual m^{-3}
A_2	0	individual m^{-3}
A_3	0	individual m^{-3}
A_4	0	individual m^{-3}
A_5	0	individual m^{-3}
A_6	0	individual m^{-3}

Table 4.3: The initial condition of the biological model.

The initial values of Z_i are calculated by multiplying A_i with the reference individual body weight of the respective life cycle stages. All *Acartia clausi* life cycle stages, phytoplankton, nutrient and detritus are homogeneously initialized in the water column.

4.4 Model results and discussion

Temperature distribution The seasonal variations of the sea temperature from the three scenarios are presented in Figure 4.2. According to Otto et al. (1990), the mean SST at the location of scenario 1 is 6.5-7°C in February and 14-14.5°C in August; at the location of scenario 2 the mean SST is around 5.5°C in February and 15-15.5°C in August; at the location of scenario 3 the mean SST is 5-5.5°C in February and 15.5-16°C in August. In the model result, the mean SST in scenario 1 is 6.8°C in February and 14.1°C in August; in scenario 2 the mean SST is 5.5°C in February and 14.5°C in August; in scenario 3 the mean SST is 5.3°C in February and 15.9°C in August. Compared to the observations, the simulated temperatures are reasonable.

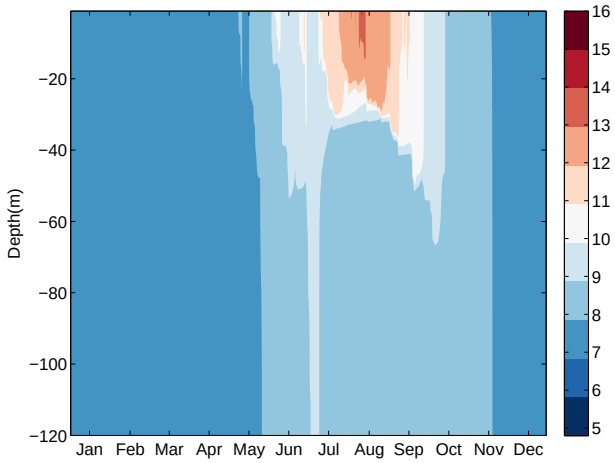

(a)

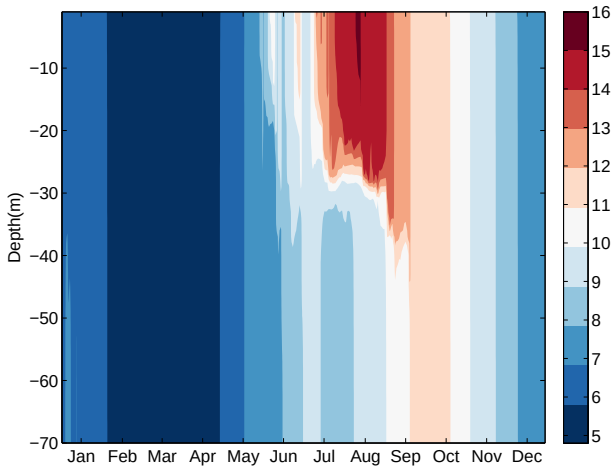

(b)

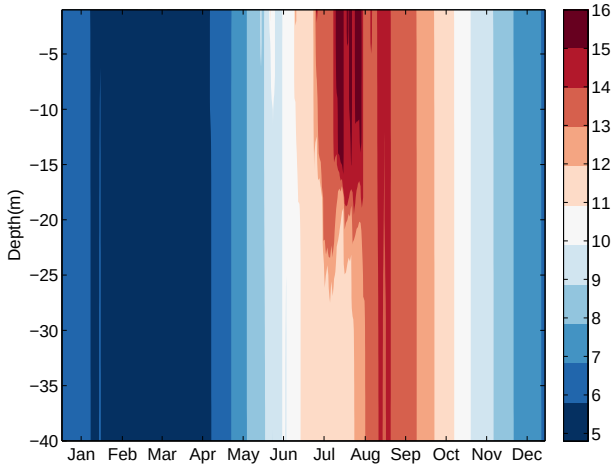

(c)

Figure 4.2: The seasonal variations of the sea temperature in scenario 1 (a), scenario 2 (b) and scenario 3 (c).

The turbulence intensity can be inferred from the vertical temperature profile. In the cold months from November to March, the water columns in the three scenarios are all well mixed. In the warm months from May to October, the increase in SST stabilizes the water column enabling the possibility of the stratification. In scenario 1 and scenario 2, temporal thermoclines form at around 20-30 m depth in summer. In scenario 3, because the water depth is only 40 m, tides and the surface heat exchange well mix the water column all through the year. The temporal thermocline is unable to form in scenario 3. The model results are reasonable compared to Otto et al. (1990) that the locations of scenario 1 and 2 are in the 'stratified' area while the location of scenario 3 is in the 'mixed' area.

Model results from DS1 and SE1 The seasonal variations of the phytoplankton biomass concentration and the abundance of different *Acartia clausi* life cycle stages are shown in Figure 4.3. At the beginning of the year, the phytoplankton biomass concentration remains at a low level (nearly 0 mmol N m^{-3}) because of the light limitation. The phytoplankton biomass concentration begins to increase from week 10 onwards. In week 22, the phytoplankton biomass concentration reaches the maximum peak of the year with the amplitude of 2.0 mmol N m^{-3}. This value is equivalent to 3.2 mg chl m^{-3} (first using the Redfield ratio and the mole to gram conversion of carbon to convert unit mmol N m^{-3} into mg C m^{-3} and then assuming that 1 mg C equals 0.02 mg chl (Radach and Pätsch, 1997)). Compared to the observation at the Stonehaven sampling station and the North Sea chlorophyll concentration distribution displayed in Radach and Pätsch (1997), the amplitude of the maximum phytoplankton biomass concentration peak in scenario 1 is in a reasonable range. Because of the combined effect of the nutrient depletion, grazing and mortality, the phytoplankton biomass concentration decreases gradually after the maximum peak. In week 35, the phytoplankton biomass concentration has decreased to less than 0.4 mmol N m^{-3}. The autumn phytoplankton bloom comes in week 36 when the vertical mixing refreshes the nutrient supply before the light availability becomes limiting. The magnitude of the autumn bloom is much smaller than that of the spring bloom, reaching only 0.7 mmol N m^{-3}. The simulated seasonal variation of the phytoplankton biomass concentration exhibits a typical northern North Sea phytoplankton distribution pattern that according to Bresnan et al. (2009), the phytoplankton biomass concentration remains low from November to the subsequent February and increases rapidly from March to June.

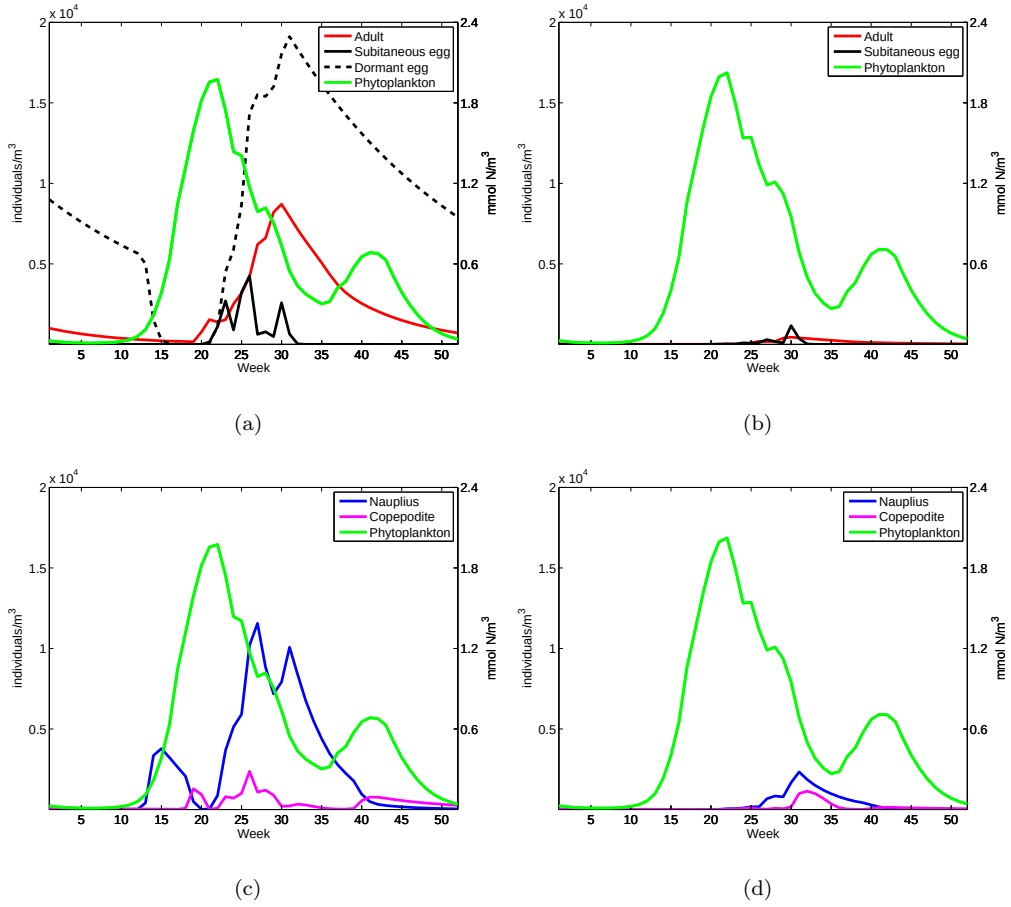

Figure 4.3: The seasonal variations of the phytoplankton biomass concentration (weekly vertically mean, right y-axis) and the abundance of different *Acartia clausi* life cycle stages (weekly vertically mean, left y-axis) in DS1 (a,c) and SE1 (b,d).

With different reproductive patterns, the seasonal variations of the abundance of different *Acartia clausi* life cycle stages in DS1 and SE1 are different. According to the model setups, dormant eggs are produced simultaneously with subitaneous eggs in DS1. After being produced, the dormant eggs stay in dormancy and the subitaneous eggs hatch in the following few days (Figure 4.3a). Subitaneous eggs hatch soon after being produced, implying that the water temperature in scenario 1 is not limiting the hatching process. The overwintering life cycle stages in DS1 are adults and dormant eggs. The dormant eggs finish the dormancy period in week 13 and begin to hatch. The newly hatched nauplii from the dormant eggs initialize the seasonal cycle of *Acartia clausi* of the year (Figure 4.3c). By feeding on the rapid increasing phytoplankton biomass, the nauplii hatched from dormant eggs develop to copepodites and form the first copepodite peak in week 17, right before the maximum phytoplankton biomass concentration peak.

This makes a tight match between *Acartia clausi* and phytoplankton. The individuals from the first cohort develops to adult in week 21, which greatly increase the abundance of spawning adults. From this time point, the abundance of *Acartia clausi* comes to the phase of fast increment. In week 31, the adult abundance reaches the annual maximum peak.

In SE1, the model setup is that *Acartia clausi* produces only subitaneous eggs. The subitaneous eggs all hatch in a few days after being produced (Figure 4.3b). The overwintering life cycle stage in SE1 are adults. The model results show that it is not until week 25 that the overwintering adults have accumulated enough biomass and begin to produce the first egg cohort, which initialize the seasonal cycle of *Acartia clausi* of the year. The timing of the first nauplius cohort in SE1 is later than that in DS1 for more than 10 weeks. The late timing of the initialization of the seasonal cycle of *Acartia clausi* causes a mismatch between *Acartia clausi* and phytoplankton. Because of this mismatch, the amplitude of the maximum adult abundance peak in SE1 is nearly 8 times smaller than that in DS1.

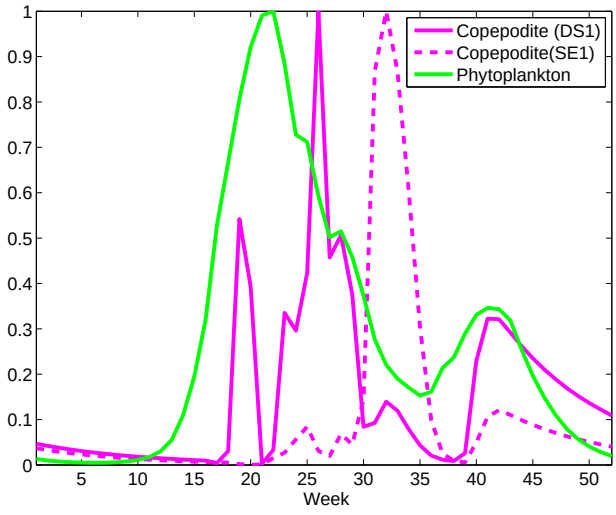

Figure 4.4: The normalized seasonal variations of the phytoplankton biomass concentration (green solid line), and the copepodite abundance in DS1 (magenta solid line) and SE1 (magenta dashed line).

Producing dormant eggs for overwintering seems to be a beneficial strategy. Dormant eggs hatching at the beginning of the year extends the growing season of *Acartia clausi* and match *Acartia clausi* with phytoplankton. Both of these two effects lead to a higher *Acartia clausi* abundance. But this tight match is not recorded at the

Stonehaven sampling station. I normalize the seasonal variations of the phytoplankton biomass concentration and copepodite abundance with their own maximum annual peaks of the year (Figure 4.4). The results show that the first copepodite cohort in DS1 appears in week 19 and its abundance can reach 55% of the maximum copepodite abundance peak in DS1 and the first copepodite cohort in SE1 appears in week 25 and its abundance reaches less than 10% of the maximum copepodite abundance peak in SE1. At the Stonehaven sampling station (Figure 2.4), the earliest timing of the chlorophyll concentration peak during the observation period is in week 15 but the chance that *Acartia clausi* copepodite abundance can reach 10% of the maximum copepodite abundance peak before week 21 is very low. In scenario 1, the timing of the phytoplankton peak is in week 21 but in DS1 the *Acartia clausi* copepodite abundance has reached 55% of the maximum copepodite abundance peak of the year in week 19. The early timing of the first copepodite cohort and its high abundance are not documented at the Stonehaven sampling station. The model results in DS1 do not fit the observed seasonal cycle of *Acartia clausi*.

Compared to the observation data, the model results from SE1 are more reasonable. In SE1, when the timing of the maximum phytoplankton peak is later than the observed earliest timing of the chlorophyll concentration peak at the Stonehaven sampling station, the timing of the first copepodite cohort is also later than the timing of the observed first copepodite cohort. And the abundance of the first copepodite cohort in SE1 is less than 10% of the maximum copepodite abundance peak of the year.

Model results from DS2 and SE2 The seasonal variations of the phytoplankton biomass concentration and the abundance of different *Acartia clausi* life cycle stages are shown in Figure 4.5. Because the location of scenario 2 is to the south of the location of scenario 1, the phytoplankton biomass concentration begins to increase earlier in scenario 2 than in scenario 1. The phytoplankton biomass concentration begins to increase from week 5 and in week 17, the phytoplankton biomass concentration reaches its maximum peak of the year (Figure 4.5). The maximum phytoplankton biomass concentration peak is nearly 2.4 mmol N m^{-3}. Because of the nutrient depletion and mortality, the phytoplankton biomass concentration decreases gradually after the maximum peak. The autumn phytoplankton bloom occurs in week 35.

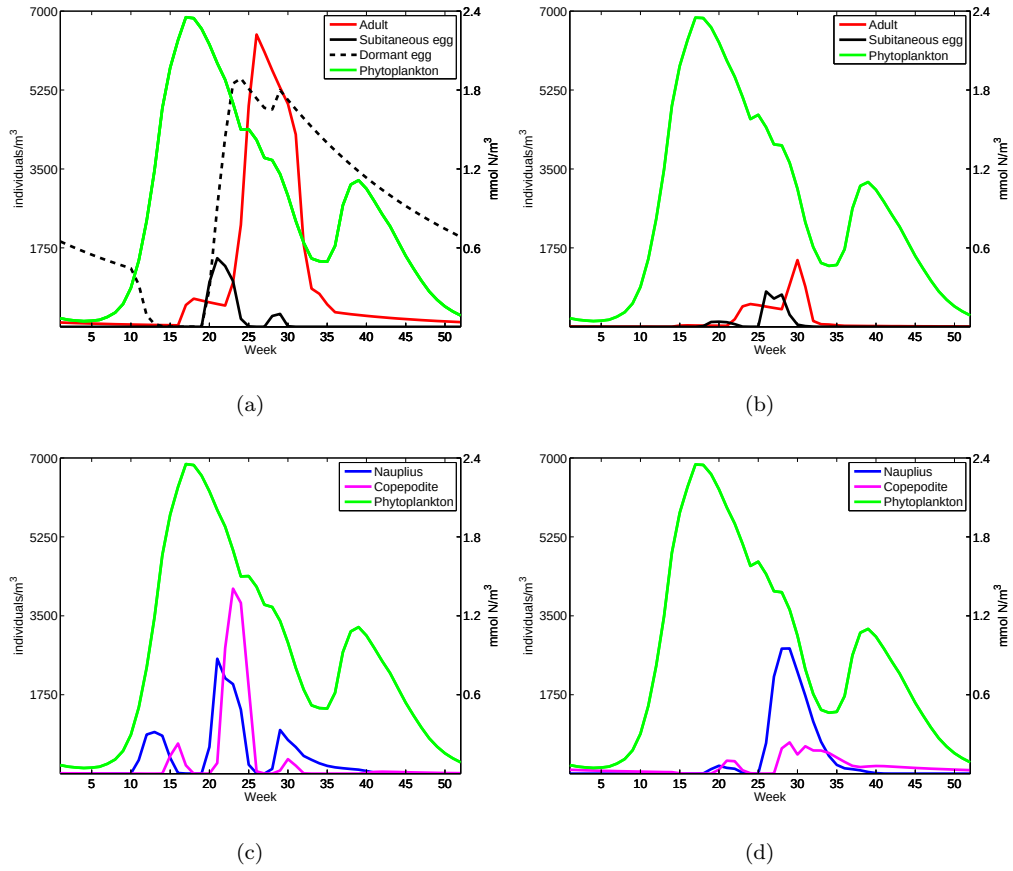

Figure 4.5: The seasonal variations of the phytoplankton biomass concentration (weekly vertically mean, right y-axis) and the abundance of different *Acartia clausi* life cycle stages (weekly vertically mean, left y-axis) in scenario 1, DS2 (a,c) and SE2 (b,d).

The seasonal variation of *Acartia clausi* abundance in DS2 is quite similar to that in DS1. Producing dormant eggs helps *Acartia clausi* to match better with phytoplankton. Before the maximum phytoplankton biomass concentration peak, the dormant eggs finish the dormancy period and hatch (Figure 4.5a). The nauplii hatched from dormant eggs initialize the seasonal cycle of *Acartia clausi* (Figure 4.5c). The individuals of the first cohort develop to the life cycle stage copepodite in week 14 before the maximum phytoplankton biomass concentration peak. By feeding on the high concentration of the phytoplankton biomass, the abundance of *Acartia clausi* increases fast. In week 26, the adult abundance reaches its maximum peak of the year.

The maximum adult abundance peak in SE2 appears in week 30 and its amplitude is 4 times smaller compared to the magnitude of the maximum adult abundance peak in DS2. The reason for this difference lies in the timing of the first *Acartia clausi* cohort

too. Taking the copepodite abundance for example, the first copepodite cohort in SE2 is about 5 weeks later than the first copepodite cohort in DS2. This delay causes the first *Acartia clausi* cohort to miss the maximum phytoplankton biomass concentration peak. But in scenario 2, the phytoplankton biomass concentration increases earlier than that in scenario 1. This leads to an earlier timing of the the first generation in SE2 than in SE1. The time lag of the first copepodite cohort between SE2 and DS2 is much smaller than the time lag of the first copepodite cohort between SE1 and DS1. For this reason, the difference of the amplitude between the maximum adult abundance peak in SE2 and DS2 is smaller than the difference between SE1 and DS1.

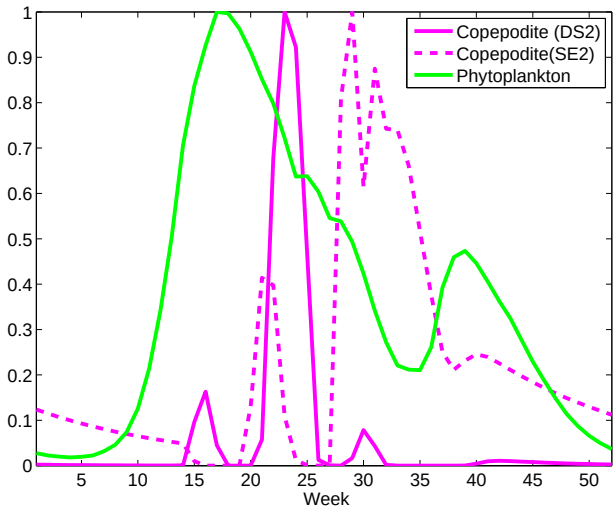

Figure 4.6: The normalized seasonal variations of the phytoplankton biomass concentration (green solid line) and the copepodite abundance in DS2 (magenta solid line) and SE2 (magenta dashed line).

The normalized seasonal variations of the phytoplankton biomass concentration and the copepodite abundance are shown in Figure 4.6. The results show that the timing of the maximum phytoplankton biomass concentration peak is in week 17. The first copepodite cohort in DS2 appears in week 14 with amplitude reaching 17% of the maximum copepodite abundance peak of the year. The first copepodite cohort in SE2 appears in week 19 and its abundance reaches 40% of the abundance of the maximum copepodite peak in SE2. Compared to the observation at the Stonehaven sampling station, the early timing of the first copepodite cohort in DS2 is not recorded and its abundance is also too high. The model result in DS2 can not reproduce the observed seasonal cycle of *Acartia clausi*. Compared to the observation, the model

results from SE2 are more reasonable. In SE2, the timing of the first copepodite cohort is in agreement with the observation.

Model results from DS3 and SE3 The seasonal variations of the phytoplankton biomass concentration and the abundance of different *Acartia clausi* life cycle stages are shown in Figure 4.7. The location of scenario 3 is near the south outlet of the North Sea. The timing of the maximum phytoplankton biomass concentration peak is the earliest among the three scenarios. The phytoplankton biomass concentration begins to increase from week 4 and reaches the maximum peak in week 14 with an amplitude of 2.4 mmol N m^{-3}. Because in summer the nutrient supply is relative sufficient due to the strong vertical mixing, the phytoplankton biomass concentration maintains at a high level (above 1.5 mmol N m^{-3}) until day 250 when the solar radiation becomes limiting.

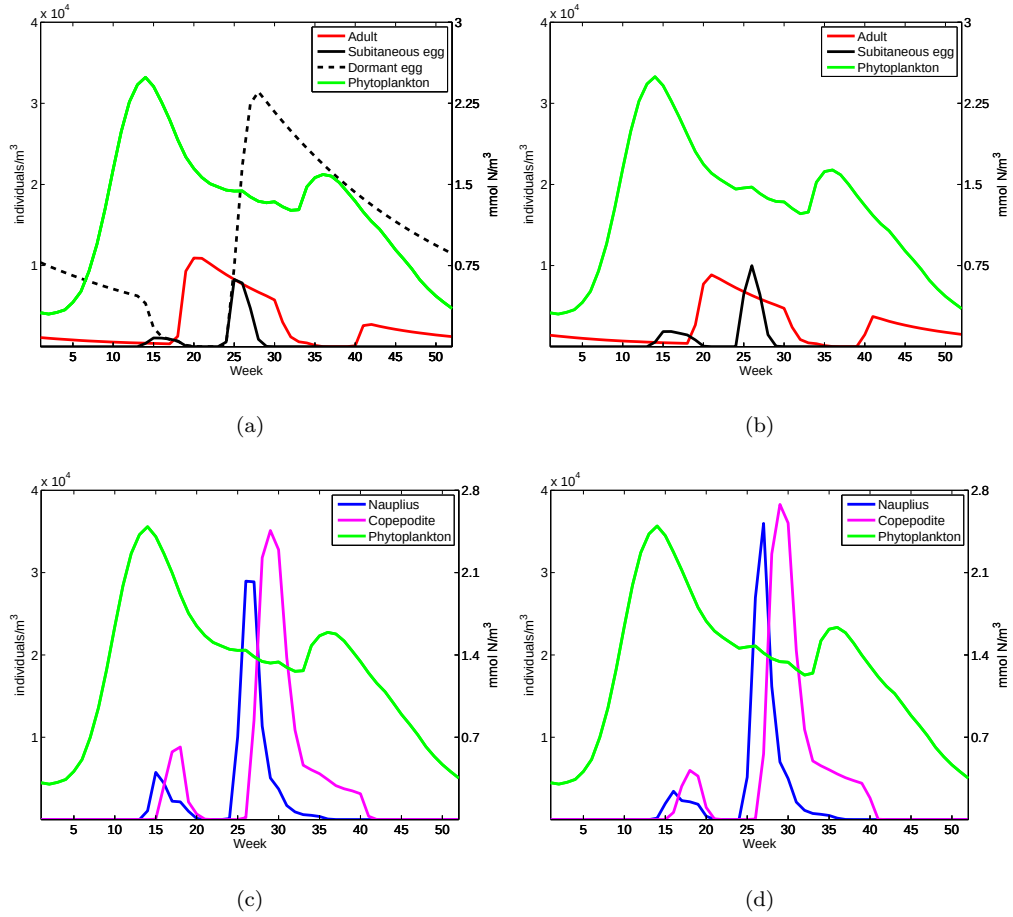

Figure 4.7: The seasonal variations of the phytoplankton biomass concentration (weekly vertically mean, right y-axis) and the abundance of different *Acartia clausi* life cycle stages (weekly vertically mean, left y-axis) in DS3 (a,c) and SE3 (b,d).

Under this special seasonal variation of the phytoplankton biomass concentration, the seasonal variations of *Acartia clausi* abundance in DS3 and SE3 are similar. In DS3, the overwintering life cycle stages are adult and dormant egg. Because the phytoplankton biomass concentration begins to increase very early, before the overwintering dormant eggs finish the dormancy period, the overwintering adults have already accumulated enough biomass and begin to produce eggs (Figure 4.7a). The hatching of the dormant eggs do not advance the timing of the first generation. Because of this reason, the timing and the amplitude of the maximum adult abundance peaks in DS3 and SE3 are very close. In DS3, the overwintering dormant eggs function just like subitaneous eggs because they hatch together with the newly produced subitaneous eggs meaning that the dormant eggs have no positive effects on the seasonal cycle but just delaying their hatching by staying in dormancy. During the period of them staying in the dormancy, a great portion of the dormant eggs are lost due to mortality. This causes negative effects on the seasonal cycle of *Acartia clausi* because a part of eggs which should be used to increase the community abundance are lost.

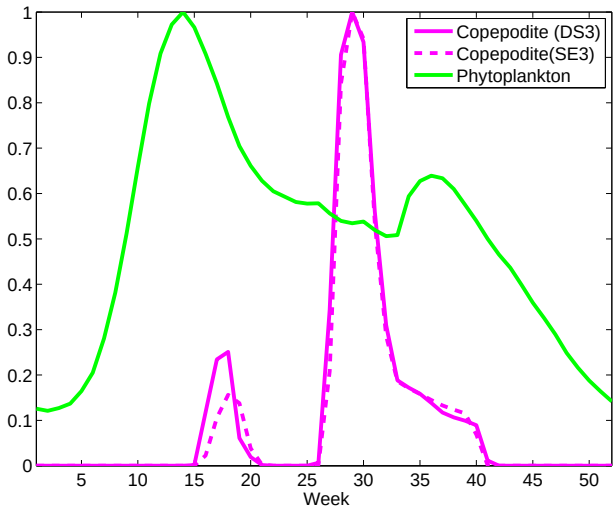

Figure 4.8: The normalized seasonal variations of the phytoplankton biomass concentration(green solid line) and the copepodite abundance in DS3 (magenta solid line) and SE3 (magenta dashed line).

The normalized seasonal variations of the phytoplankton biomass concentration and copepodite abundance are shown in Figure 4.8. The results show that the timing of the first copepodite cohort in DS3 and in SE3 are the same, all in week 15.

4.5 Summary and conclusion

In this chapter, I model the seasonal variation of *Acartia clausi* abundance under different reproductive patterns in three scenarios. Specifically, I focus on the dormant egg production because *Acartia clausi* may produce dormant eggs for overwintering. The model results show that seeing from the timing of the maximum phytoplankton biomass concentration peak, the dormant eggs function in two ways. The first is that in the northern and central North Sea, producing dormant eggs for overwintering helps *Acartia clausi* to match better with phytoplankton by extending the growing season of *Acartia clausi*. The second is that in the southern North Sea, producing dormant eggs has negative influences on the seasonal cycle of *Acartia clausi*. In DS3, the dormant eggs finish the dormancy period after the timing of the maximum phytoplankton biomass concentration. At the time when dormant eggs hatch, overwintering adults have already begun to produce eggs. The hatching of dormant eggs does not help *Acartia clausi* to match better with phytoplankton. The adverse effect of producing dormant eggs is that a portion of dormant eggs are lost in vain during dormancy period because of mortality.

I compare the model results from scenario 1 and scenario 2 to the observation at the Stonehaven sampling station and find that the seasonal variations of *Acartia clausi* abundance in DS1 and DS2 can not reproduce the observed seasonal cycle of *Acartia clausi*. The seasonal variations of *Acartia clausi* abundance in SE1 and SE2 are more in agreement with the observation. This means that in the northern and central North Sea, producing dormant eggs should not be included in the model as an overwintering strategy.

In the southern North Sea, Wesche et al. (2007) studied the overwintering strategy of *Acartia clausi* in the German Bight. They did not find that in this area *Acartia clausi* produced dormant eggs for overwintering and the main overwintering life cycle stage of *Acartia clausi* was adult. The model results from scenario 3 show that when overwintering dormant eggs hatch after the maximum phytoplankton biomass concentration peak, the seasonal variation of *Acartia clausi* abundance differs little with or without considering producing dormant eggs as an overwintering strategy.

Thus, I come to the conclusion that when modelling the seasonal variation of *Acartia clausi* abundance in the North Sea, it is not necessary to include the dormant egg production into the life cycle model as an overwintering strategy.

Chapter 5

Contemporary and projected phenological patterns of phyto-zooplankton in the North Sea

5.1 Motivation

Copepods play an important role in many marine ecosystems as grazers, providing an important pathway for energy from primary producers to consumers at higher trophical levels. Changes in the copepod abundance due to climate variations are observed to affect the abundance of fishes and induce regime shifts in marine ecosystems (e.g., Beaugrand et al., 2003; Alheit et al., 2005; Möllmann et al., 2008). The seasonal development of the copepod abundance depends on the temporal match between copepods and their food source: phytoplankton. Phenology, or the life cycle dynamics of plankton (zooplankton and phytoplankton), is very sensitive to climate variations because temperature is a key parameter affecting the growth rate, body size and generation time of plankton. Phenological changes of plankton caused by climate variations have been reported in different marine ecosystems (e.g., Mackas et al., 1998; Edwards and Richardson, 2004). It is assumed that in the future, climate warming will disturb the temporal match between copepods and phytoplankton if they fail to response to future climate warming synchronously. The decoupling of the phenological patterns may cause a decline in the copepod abundance through bottom-up effects. One concern is

that the signal will resonate to upper trophic levels, affecting the yields of commercially important fishes.

The aim of this part is to project the potential phenological changes of phytoplankton and copepods caused by future climate warming and to see whether future climate warming will induce a temporal mismatch between them. In this chapter, I focus on the North Sea and the key North Sea copepod species, *Acartia clausi*. Throughout the North Atlantic Ocean, a general increase in SST has been recorded in the past century (Beaugrand, 2009). This warming trend is projected to continue in the future. The North Sea is a marginal sea of the North Atlantic Ocean. The sea temperature in the North Sea is also observed to increase, e.g. since 1981 there has been a documented increase of 0.2-0.4°C per decade in SST in the northwestern North Sea (Fisheries Research Services, 2003). In the future, according to the projections of the GCMs 'HadCM3' (Gordon et al., 2000; Pope and Macer, 1996), the annual mean SST of the North Sea will increase from 10.3°C (annual mean SST 1990-1999) to 10.7-11.5°C until 2050, and by the end of 21st century, according to IPCC (2007), the annual mean SST of the North Sea is projected to be increased by 1.5-3.5°C.

In this chapter, I project the phenological responses of phytoplankton and *Acartia clausi* to climate warming, and study the interaction between phytoplankton and *Acartia clausi* in a warmer environment through modelling the seasonal variations of phytoplankton biomass concentration and *Acartia clausi* abundance based on the projected temperature rises in the North Sea. In detail, two steps in this study are conducted. Firstly, the ecosystem model is applied to reproduce the seasonal variations of phytoplankton biomass concentration and *Acartia clausi* abundance at the Stonehaven sampling station aiming to get an overview of the contemporary phenological pattern of phytoplankton and *Acartia clausi*, and also to get a better understanding of the life cycle dynamics of *Acartia clausi* in the North Sea. The first step at the same time provides a comparable counterpart for the following warming scenarios. Secondly, I model the seasonal variations of phytoplankton biomass concentration and *Acartia clausi* abundance based on the projected North Sea temperature rises.

5.2 Ecosystem model

In this chapter, I couple the life cycle model of *Acartia clausi* to a nitrogen based Phytoplankton-Nutrient-Detritus (PND) model by replacing the bulk zooplankton compartment (Z) in the PNZD model with the life cycle model of *Acartia clausi*. The equation system and parametrizations of the biological processes in the biological model are basically the same with those in Chapter 3 and Chapter 4 except that in this chapter I parametrize a temperature limitation for the phytoplankton growth in order to take into account the effects of climate warming on the development of the phytoplankton biomass concentration.

PND model setup Phytoplankton is the prime producer of the marine ecosystem. A reasonable numerical representation of the observed seasonal variation of the phytoplankton biomass concentration is the prerequisite for reproducing the observed seasonal variation of *Acartia clausi* abundance. In addition to light and nutrient, temperature is also regarded as a limiting factor for the phytoplankton growth. It is observed that there is an optimum temperature for algae growth. The growth rate of algae increases gradually at suboptimal temperatures and decreases at supraoptimal temperatures (Eppley, 1972). I use a Gaussian function to parametrize the temperature limitation on the phytoplankton growth rate. The growth rate of phytoplankton is calculated in this chapter with the equation:

$$\begin{aligned} \mu_P &= \mu_{P_{max}} \frac{I_{par}}{max(I_0/4, I_{min})} \exp\left(1 - \frac{I_{par}}{max(I_0/4, I_{min})}\right) \frac{N_u}{k_{N_u} + N_u} \\ &\quad \exp(-\frac{(T - T^P_{opt})^2}{(T^P_{scale})^2}) \end{aligned} \tag{5.1}$$

In Equation 5.1, only the temperature limitation is newly implemented, the other parts of this equation have already been introduced in Chapter 4. The term T^P_{opt} is the optimal temperature for the phytoplankton growth and T^P_{scale} is a reference temperature. The value of T^P_{opt} is given referring to Thomas et al. (2012) in which the relation between optimal temperatures for the phytoplankton growth and annual mean SST of the sea regions where phytoplankton reside are compiled from observation data. The annual mean SST at the Stonehaven sampling station during the observation period is 9.6°C. According to compiled information in Thomas et al. (2012), I set the value of T^P_{opt} to be 16°C.

The parameter values used in the PND model are listed in Table 5.1.

Parameters	value	unit
$\mu_{P_{max}}$	2.2	d^{-1}
r_{par}	0.35	-
I_{min}	35	W m^{-2}
k_w	0.05	m^{-1}
k_c	0.06	m^{-2} mmol N^{-1}
k_{N_u}	1.2	mmol N m^{-3}
η_P	0.02; 0.05*	d^{-1}
γ	0.014	d^{-1}
l_P	0.01	d^{-1}
w_{D_l}	-5	m d^{-1}
w_{D_s}	-0.3	m d^{-1}
w_P	-1	m d^{-1}
φ	30%	-
T^P_{opt}	16	°C
T^P_{scale}	11	°C

Table 5.1: The parameter values in the PND model of Chapter 5 (*: The phytoplankton mortality rate in euphotic zone is smaller than that below the euphotic zone).

Parameter values in the life cycle model of *Acartia clausi* In Chapter 4, I find that it is not necessary to take the dormant egg production into account as an overwintering strategy when modelling the life cycle dynamics of *Acartia clausi* in the North Sea. In this chapter, I use the life cycle model of *Acartia clausi* in Chapter 4 and set that all the produced eggs are subitaneous eggs. Here, I increase the constant mortality rates of some life cycle stages so that the model can reproduce the seasonal variation of *Acartia clausi* abundance measured at the Stonehaven sampling station. In Table 5.2, the parameter values of the life cycle model are listed.

Parameters	Z_1	Z_2	Z_3	Z_4	Unit
Ingestion					
$g_{i\max_P}$	-	2.8	1.8	0.58	d^{-1}
$g_{i\max_D}$	-	5.6	3.6	1.16	d^{-1}
k_P	-	2.0	2.0	2.0	mmol N m^{-3}
k_{D_s}	-	5.0	5.0	5.0	mmol N m^{-3}
α	-	3.5	3.5	3.5	-

Continued on next page

Table 5.2 – Continued from previous page

Parameters	Z_1	Z_2	Z_3	Z_4	Unit
T_{opt}	-	15	15	15	°C
T_1	-	1	1	1	°C
T_2	-	7	7	7	°C
Reproduction					
k_{w_4}	-	-	-	5.0e-06	mmol N ind^{-1}
δ	-	-	-	0.25	d^{-1}
ρ_{fem}	-	-	-	80%	-
ε_j	100%	-	-	-	-
Moulting					
k_{w_i}	-	1.02e-06	1.18e-06	-	mmol N ind^{-1}
Hatching					
T_{scale}	20	-	-	-	°C
n	0.1085	-	-	-	°C^{-1}
Egestion and excretion					
β_P	-	0.77	0.77	0.77	-
β_{D_s}	-	0.16	0.16	0.16	-
ς_i	-	10.5%	5.5%	4.4%	d^{-1}
$Q10$	-	2.58	2.58	2.58	d^{-1}
T_{ref}	-	10	10	10	°C
Mortality					
f_{c_i}	-	9.5	9.5	9.5	-
r_{max}	100%	100%	100%	100%	d^{-1}
r_i	15%	4.0%	3.6%	3.6%	d^{-1}
ω_i	0	1	1	1	-
Vertical velocity (assuming upward velocity as positive)					
w_{Z_i}	-20	0.5	1	1.5	m d^{-1}

Table 5.2: The parameter values in the life cycle model of *Acartia clausi* in Chapter 5.

5.3 Model setups and application

5.3.1 Model setups

The one-dimensional water column model, GOTM is used as the framework for the hydrodynamics at the Stonehaven sampling station and for the coupling of biology and physics. Referring to the water depth at the Stonehaven sampling station, the vertical depth in the model is set to be 50 m. The vertical resolution of the physical model is one meter per level. The time step is one hour.

Physical model setup The physical model is initialized with temperature and salinity vertical profiles. The wind speed at 10 m height above the sea surface and the sea surface slope gradient in zonal and meridional directions are applied as forcing. The air temperature and relative humidity at 2 m height above the sea surface together with surface air pressure are applied to calculate the sea surface momentum and heat flux with the formular from Kondo (1975). I use the second order model as the turbulence closure. The turbulent kinetic energy and the dissipative length scale are calculated in k-epsilon style. The type of the stability function is set referring to Schumann and Gerz (1995). The values of the coefficients in the second order model are set referring to Cheng et al. (2002), and the parameter values in the k-epsilon model are given according to Rodi (1987).

The salinity and temperature profiles are from a high resolution 3D North Sea circulation model (HAMSOM) (Chen et al., 2012). Based on the salinity and temperature data from Chen et al. (2012), which are daily mean values from 1970-2001, I generate a climatological daily mean salinity and temperature time series data for one year. The meteorological data such as wind speed, relative humidity, cloud coverage and air temperature are from NCEP/NCAR reanalysis 1 (Kalnay et al., 1996) daily mean data. I take the daily mean meteorological data from 1970-2001 and generate a climatological daily mean time series data for one year. In order to produce a meteorological forcing with the temporal resolution of 6 hours, I interpolate linearly between the climatological daily mean values. The surface air pressure in the model are assumed to be constant as 101.3 kPa. The surface slope gradient data are taken from the GOTM scenario 'Annual North Sea Simulation' (Burchard, 1999; Bolding et al., 2002), which are generated from observations during autumn 1998 based on the harmonic analysis of

four partial tides. The internal pressure gradients are set to zero. I repeat the forcing every model year.

Ecosystem model setup The ecosystem model is resolved with the second-order modified Patankar-Runge-Kutta scheme. The time step and the vertical resolution of the biological model are set to be the same as in the physical model. The initial conditions of the biological model are homogeneously applied to all the water levels at the beginning of the simulation. The initial conditions of the biological model compartments are listed in Table 5.3. The value of the initial nutrient concentration (N_u) is given based on the observation that in winter at surface layer, the nitrate concentration at Stonehaven is 5.5-14.5 mmol N m^{-3} (Bresnan et al., 2009). Since in winter the water column is well mixed, the nitrate concentration at each depth level should be the same.

Parameter	value	unit
P	0	mmol N m^{-3}
N_u	5.5	mmol N m^{-3}
D_l	4.5	mmol N m^{-3}
D_s	0	mmol N m^{-3}
A_1	10000	individual m^{-3}
A_2	0	individual m^{-3}
A_3	0	individual m^{-3}
A_4	0	individual m^{-3}
A_5	0	individual m^{-3}
A_6	0	individual m^{-3}

Table 5.3: The initial conditions of the biological model in Chapter 5.

5.3.2 Model applications

I have conducted five simulations including one 'standard' model simulation and four warming scenarios. In the 'standard' model simulation, the ecosystem model is applied to reproduce the seasonal variation of *Acartia clausi* abundance at the Stonehaven sampling station. For convenience, I label it as TR0 (annual mean Temperature is Raised by 0°C). Following, four warming scenarios are conducted based on the projected future North Sea annual mean SST rises. The model setup for the four warming scenarios are the same as in the 'standard' model simulation, except the altered temperature forcing. The annual mean SST in the four warming scenarios are increased by 1.2°C, 2°C, 2.5°C

and 3°C, respectively. For convenience, I label them as TR1.2, TR2, TR2.5 and TR3. TR1.2 is designed according to the output from the GCMs 'HadCM3' that until 2050 the annual mean SST in the North Sea will be increased by 0.4-1.2°C. I take the larger value for the first warming scenario. The other three warming scenarios are designed based on the projection from the IPCC (2007) that until the end of the 21st century, in the low greenhouse gas emission scenario the annual mean SST in the North Sea will be increased by 1.5-2°C, and in the high emission scenario by 2-3.5°C.

5.4 Model results

5.4.1 Seasonal variations of SST and the phytoplankton biomass concentration

Seasonal variation of SST The seasonal variations of SST from TR0 and the Stonehaven sampling station are shown in Figure 5.1. In the model result, the annual lowest SST is in March with the value of 6.1°C and the annual highest SST is in September with the value of 12.6°C. At the Stonehaven sampling station, the annual minimum SST occurs, on average, in late February/early March with the value of around 6°C, and the annual maximum SST occurs during August/September with the value of 12-14°C. The model result is in agreement with the observation in timing and values of the annual lowest and highest SST. Only in the summer months (July/August), the simulated temperature is slightly lower than the observed temperature.

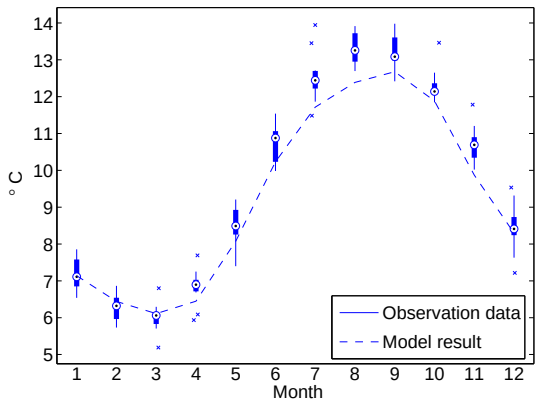

Figure 5.1: The monthly mean SST from TR0 (dashed line) and the Stonehaven sampling station (box-and-whisker plot).

Seasonal variation of the phytoplankton biomass concentration The seasonal variations of the surface phytoplankton biomass concentration in TR0 and the surface chlorophyll concentration at the Stonehaven sampling station are shown in Figure 5.2. In the model result, the phytoplankton biomass concentration begins to increase from week 10 and the timing of the maximum phytoplankton biomass concentration peak is in week 21. The amplitude of the maximum phytoplankton biomass concentration peak is 3.2 mmol N m^{-3}. After week 21, because of the nutrient depletion and mortality, the surface phytoplankton biomass concentration decreases rapidly and in week 26, the simulated surface phytoplankton concentration has decreased to nearly 1 mmol N m^{-3}. From week 26, because more recycled nutrients from the remineralization of detritus and excretion of *Acartia clausi* are available for the phytoplankton growth, the phytoplankton concentration exhibits a smaller peak in week 29. After week 29, the phytoplankton biomass concentration decreases monotonically to the minimum level of the year.

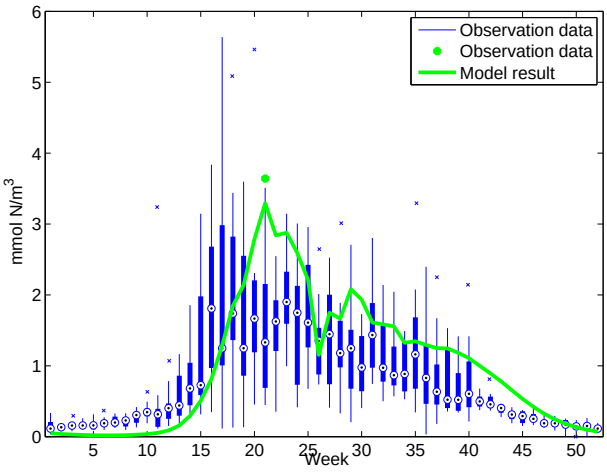

Figure 5.2: The seasonal variation of the surface chlorophyll concentration (box-and-whisker plot) and the climatological mean timing and amplitude of the surface chlorophyll concentration at the Stonehaven sampling station (green dot), and the seasonal variation of the surface phytoplankton biomass concentration in TR0 (green solid line). The unit of the surface chlorophyll concentration (mg chl m^{-3}) in the dataset is converted to mmol N m^{-3} assuming that 1 mg chl equals to 50 mg C (Radach and Pätsch, 1997) and using the gram to mole conversion of carbon and the Redfield ratio.

The general pattern of the observed seasonal variation of the surface chlorophyll concentration is that the surface chlorophyll concentration begins to increase from week 11 onwards and reaches a high level during the time period from week 16 to week 25. From week 25, the observed surface chlorophyll concentration decreases gradually. After week 40, the observed surface chlorophyll concentration is less than 0.5 mmol N m^{-3}. The climatological mean timing of the maximum surface chlorophyll concentration at the Stonehaven sampling station is in week 21 and its amplitude is nearly 3.7 mmol N m^{-3}.

The model results are able to reproduce the observed climatological mean timing of the surface chlorophyll concentration, and the amplitude of the maximum phytoplankton biomass concentration peak in the model result is close to the observed climatological mean amplitude of the maximum chlorophyll concentration peak.

At the beginning of the growing season, the surface phytoplankton concentration in TR0 begins to increase 1 week earlier than the observed timing of the rapid increase in the chlorophyll concentration. From the beginning of the year to week 12, the simulated surface phytoplankton biomass concentration is lower than the observed

chlorophyll concentration. The reason for the differences is that in the current model, the life cycles of different algae species are not considered and different algae species are treated with one bulk model compartment. It is observed that some algae species (e.g., dinoflagellates) stay in dormancy during winter as resting cysts. At the beginning of the year, these resting cysts develop into vegetative cells (Warns et al., 2013). When these biological processes of phytoplankton species are not considered in the model, the phytoplankton biomass concentration in winter and the correct timing of the phytoplankton spring bloom are not correctly simulated.

5.4.2 Seasonal variation of *Acartia clausi* abundance

Seasonal variations of copepodite and adult abundance The seasonal variations of copepodite and adult abundance from observation and TR0 are shown in Figure 5.3. In observation, the climatological mean timing of the maximum copepodite abundance peak is in week 29 and the mean timing of the maximum adult abundance peak is in week 30. In model results from TR0, the maximum copepodite abundance peak occurs in week 30 and the maximum adult abundance peak in week 31. The timing of the maximum abundance peak of the two life cycle stages in TR0 and observation are very close with only 1 week time lag.

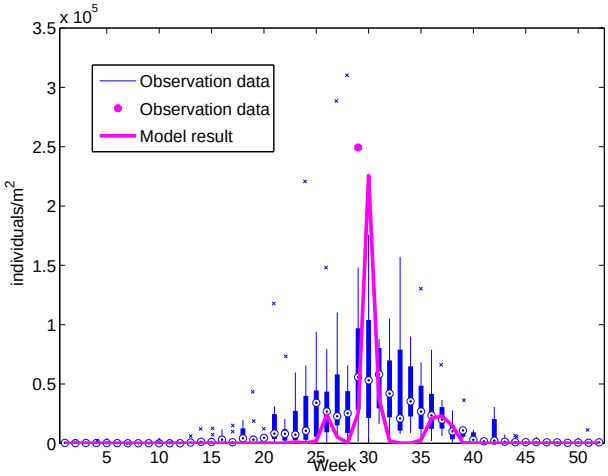

(a)

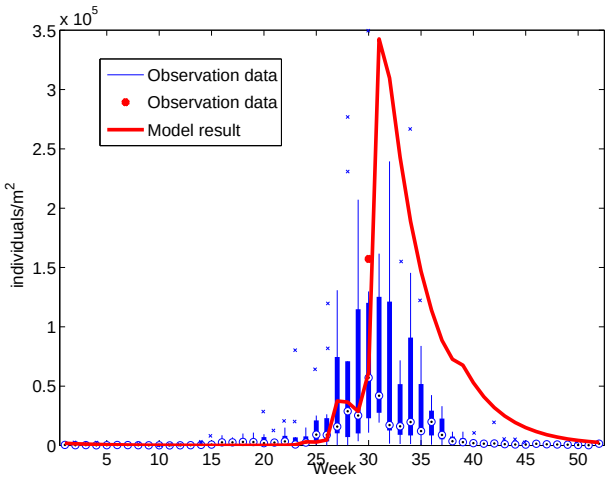

(b)

Figure 5.3: The seasonal variation of the copepodite abundance (box-and-whisker plot) and the climatological mean timing and amplitude of the maximum copepodite abundance peak (magenta dot) at the Stonehaven sampling station, and the seasonal variation of the copepodite abundance in TR0 (magenta solid line) (a); The seasonal variation of the adult abundance (box-and-whisker plot) and the climatological mean timing and amplitude of the maximum adult abundance peak (red dot) at the Stonehaven sampling station, and the seasonal variation of the adult abundance in TR0 (red solid line).

The magnitude of the maximum copepodite abundance peak in TR0 is about 0.2×10^5 individuals m^{-2} smaller than the observed climatological mean amplitude of the maximum copepodite abundance peak, and the magnitude of the maximum adult abundance peak in TR0 is two times larger than the observed climatological mean amplitude of the maximum adult abundance peak. One reason for the difference is

that the mortality rate in the model can not be properly parametrized because the mechanism regulating the mortality rate in the natural environment has not been well understood. In the observation, the magnitude of the maximum copepodite abundance peak is larger than the magnitude of the maximum adult abundance peak, implying that *Acartia clausi* abundance is heavily diminished during the ontogenetic development from copepodite to adult. This decrease in the abundance is probably caused by the increase in the mortality rate due to high predatory pressure. The predatory pressure of copepods varies with seasons. In autumn, the combination of higher water temperatures, and the higher abundance of fish larvae in the North Sea makes the local depletion of copepods by predation more likely (Nielsen and Munk, 1998). In the model the predatory pressure is parametrized with a constant mortality rate. This model design with the respect to the mortality rate is still not sophisticated enough. In the life cycle model, with more and more individuals succeeding in developing to the adulthood, the abundance of adult is greatly increased. When the mortality rate during this time is underestimated, an overestimation of the adult abundance could happen.

At the beginning of the growing season, the observation shows that from week 24, there is a large increase in the copepodite abundance. The first copepodite cohort in the observation appears in week 25. The model is consistent with the observation in the timing of the first copepodite cohort. Besides, the model is also consistent with the observation that from week 1 to week 20 and from week 40 to week 52, the copepodite abundance is at a low level.

The observed seasonal variation of the adult abundance show that the adult abundance begins to increase from week 25. In TR0, the adult abundance begins to increase from week 26. In the observation, after the time with the maximum adult abundance, the adult abundance shows a steep decrease and around week 38, the adult abundance is diminished to a very low level. In TR0, the decreasing trend of the adult abundance is not that steep as in the observation but the adult abundance decreases to a low level before the end of the year. The reason for this slow decrease of the adult abundance in TR0 is that the magnitude of the maximum adult abundance peak is too high and the mortality rate is underestimated.

Life cycle dynamics of *Acartia clausi* in the North Sea Since the model results from TR0 can reasonably reproduce the observed seasonal variation of the copepodite

and adult abundance in the timing of the maximum abundance peak and timing of the onset of the abundance increase, I use the model results from TR0 to study the life cycle dynamics of *Acartia clausi* in the North Sea.

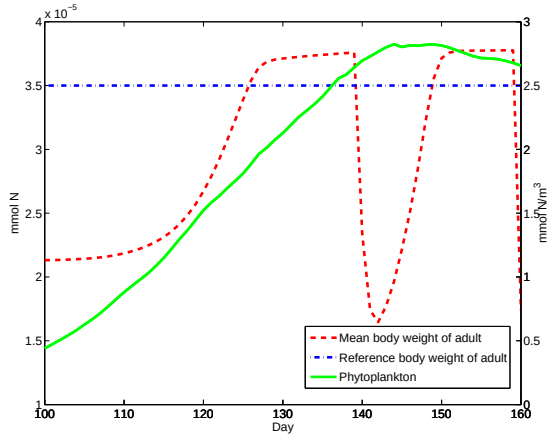

(a)

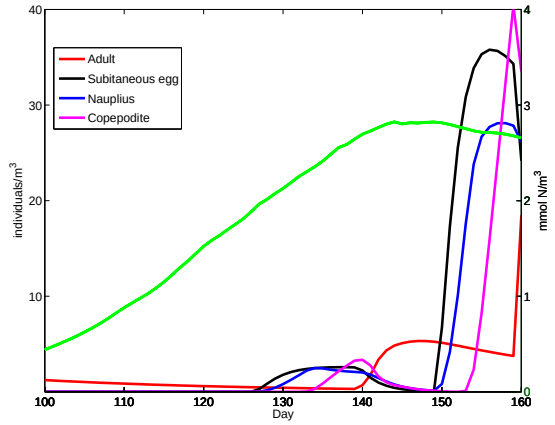

(b)

Figure 5.4: The individual body weight of adult (dashed line, left y-axis), the reference body weight of adult for reproduction (dash-dotted line, left y-axis) and the phytoplankton biomass concentration (vertically mean value, right y-axis) from day 100-160 (a); The seasonal variations of the abundance of different life cycle stages (vertically averaged value, left y-axis) and the phytoplankton biomass concentration (vertically averaged value, right y-axis) from day 100-160 (b).

Figure 5.4 elaborates the initialization of seasonal cycle of *Acartia clausi*. The seasonal cycle of *Acartia clausi* is initialized by the overwintering adults. The adults begin to produce the first egg cohort on day 127 when the mean body weight of adult

exceeds the reference body weight of adult for reproduction. At this moment the phytoplankton concentration has reached 2 mmol N m^{-3}, which applies sufficient food for the development of the first cohort. The individuals from the first generation develop to the adulthood around day 140, which greatly increases the adult abundance. From day 150, the adults begin to produce the second egg cohort. Since there are more adults producing eggs now, the abundance of the second egg cohort is much larger than that of the first egg cohort. One cohort after another, the *Acartia clausi* community is becoming more and more abundant.

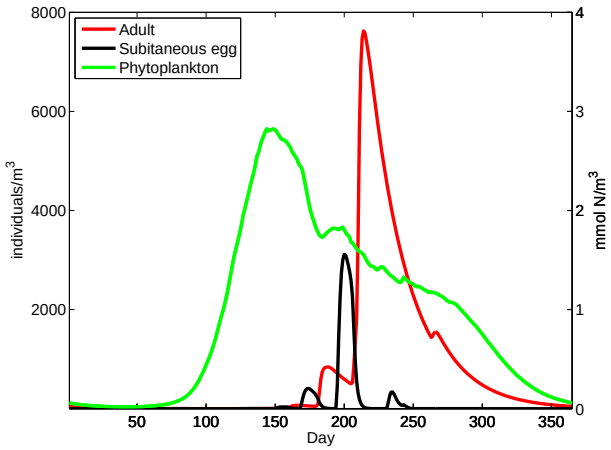

(a)

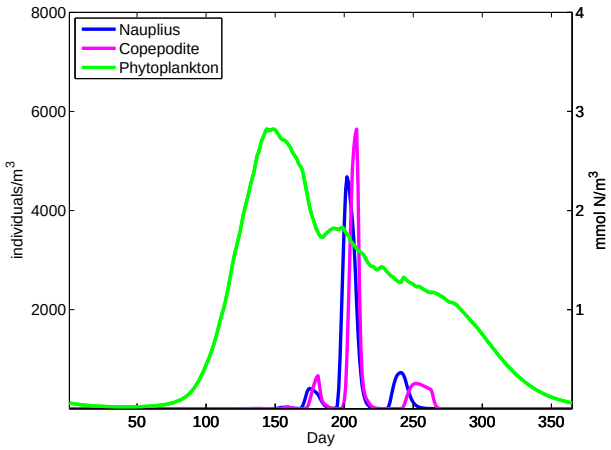

(b)

Figure 5.5: The seasonal variations of the phytoplankton biomass concentration (vertically averaged daily mean value, right y-axis) and the abundance of different *Acartia clausi* life cycle stages (vertically averaged daily mean value, left y-axis) in TR0.

There are several *Acartia clausi* cohorts during the year. Seeing from the egg abundance (Figure 5.5), before the maximum adult abundance peak there are mainly three cohorts (on day 150, day 170 and day 195). The abundance of these cohorts increases in sequence. When most of the individuals from the three cohorts develop to the adulthood, the adult abundance reaches its maximum peak of the year.

5.4.3 Responses of phytoplankton and *Acartia clausi* to climate warming

After TR0, four warming scenarios are conducted. The model results from TR0, TR1.2, TR2 and TR2.5 are shown in Figure 5.6. The model results from TR3 are not plotted in this figure, because *Acartia clausi* abundance in TR3 has decreased to less than 1 individual m^{-3}, which means that this species dies out when temperature is increased by 3°C. Detailed information about the results of the four warming scenarios are summarized in Table 5.4 and Table 5.5.

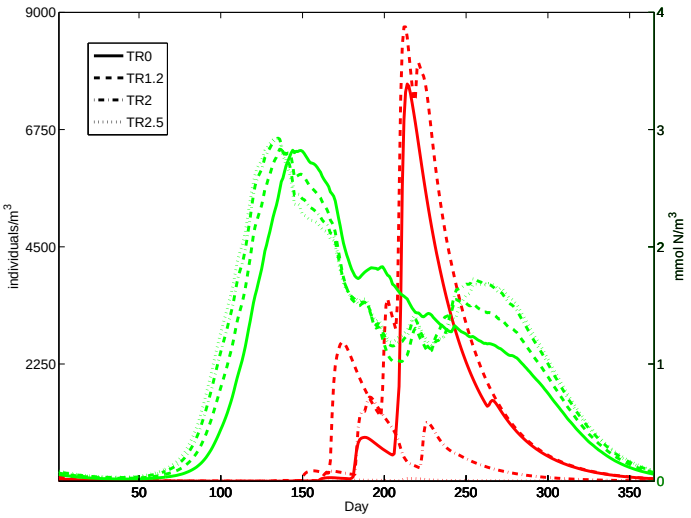

Figure 5.6: The seasonal variations of the phytoplankton biomass concentration (vertically averaged daily mean value, green color, right y-axis) and the adult abundance (vertically averaged daily mean value, red color, left y-axis) from different simulations. The model results from different simulations are shown with different line types. The model results from TR0 are plotted with solid line, from TR1.2 with dashed line, from TR2 with dash-dotted line and from TR2.5 with dotted line.

Scenarios	annual mean SST	timing of MPP	magnitude of MPP
TR0	9.11°C	day 144	2.82 mmol N m^{-3}
TR1.2	10.31°C	day 136	2.83 mmol N m^{-3}
TR2	11.18°C	day 135	2.92 mmol N m^{-3}
TR2.5	11.60°C	day 135	2.93 mmol N m^{-3}
TR3	12.06°C	day 133	2.91 mmol N m^{-3}

Table 5.4: The annual mean SST, timing of MPP (the Maximum Phytoplankton biomass concentration Peak) and magnitude of MPP from TR0, TR1.2, TR2, TR2.5 and TR3. The phytoplankton biomass concentration presented are vertically averaged values.

Scenarios	timing of first egg cohort	timing of MAP	magnitude of MAP
TR0	day 127	day 214	7.62×10^3 individuals m^{-3}
TR1.2	day 119	day 212	8.72×10^3 individuals m^{-3}
TR2	day 115	day 191	1.61×10^3 individuals m^{-3}
TR2.5	day 135	day 215	54 individuals m^{-3}
TR3	-	-	< 1 individuals m^{-3}

Table 5.5: The timing of the first egg cohort, timing of MAP (the Maximum Adult abundance Peak) and magnitude of MAP from TR0, TR1.2, TR2, TR2.5 and TR3. The adult abundance presented are vertically averaged values.

Responses of phytoplankton to climate warming When the annual mean SST is increased by 1.2°C compared to the current level (from TR0 to TR1.2), the timing of the maximum phytoplankton biomass concentration peak is advanced by 8 days. But when the annual mean SST gets even higher (in TR2, TR2.5 and TR3), the advance in the timing of the maximum phytoplankton biomass concentration peak becomes less apparent. From TR1.2 to TR3, the maximum phytoplankton biomass concentration peak is advanced by only 2 days. The variation in the timing of the maximum phytoplankton biomass concentration peak is controlled by the increases in the sea temperature as well as the light limitation because photosynthesis depends on the solar shortwave irradiance. The latitude of the Stonehaven sampling station is 56°57.8'N. Light availability is an important limitation factor for the phytoplankton growth. Hence, the timing of the maximum phytoplankton biomass concentration peak is advanced only to a certain extent by climate warming until the light limitation prevents an earlier peak even if the annual mean SST continues to rise. The magnitude of the maximum phytoplankton concentration peak exhibits less apparent changes with the annual mean SST rises. From TR0 to TR3 the biomass concentration of the maximum phytoplankton peak is increased only by 0.09 mmol N m^{-3}.

Responses of *Acartia clausi* to climate warming The responses of *Acartia clausi* to temperature rises are much more complex. Here, I use the timing of the first egg cohort to date the timing of the onset of the seasonal cycle of *Acartia clausi*.

The environmental conditions seem to become more favorable for *Acartia clausi* when the annual mean SST is increased by 1.2°C compared to the current level. In TR1.2, the first egg cohort is produced 8 days earlier compared to the timing of the first egg cohort in TR0 because the overwintering adults in TR1.2 are able to accumulate enough biomass by feeding on the earlier development of the phytoplankton biomass concentration. The magnitude of the maximum adult abundance peak in TR1.2 is about 1.1×10^3 individuals m^{-3} more than that in TR0. The reason for the increase in the adult abundance is that in TR1.2, the onset of the seasonal cycle of *Acartia clausi* is advanced and the growing season of *Acartia clausi* gets longer. In TR1.2, higher temperature better matches *Acartia clausi* with phytoplankton.

When the annual mean SST is increased by 2°C or more, the adverse effect of the rising temperature on the *Acartia clausi* appears. The adverse effect is exhibited through the decreases in the adult abundance. In TR2, although the timing of the first egg cohort is earlier than that in TR1.2 for 2 days, the amplitude of the maximum adult abundant peak is decreased by more than 65% compared to the amplitude of the maximum adult abundant peak in TR1.2. In the following two warming scenarios, TR2.5 and TR3, *Acartia clausi* experiences even worse situations. The abundance of the maximum adult peak is diminished to a very low level.

The reason for the decrease in the abundance of *Acartia clausi* when the annual mean SST is increased by more than 2°C is that the temporal match between phytoplankton and *Acartia clausi* is disturbed. The rising sea temperature increases the excretion rate of the overwintering adults. At the same time, due to the light limitation, the phytoplankton biomass concentration in winter is very low. The combined effect of the low food concentration and the high excretion rate increases the mortality rate of the overwintering adult through the starvation effect. The mean mortality rate of adult in November-April and May-October from TR0, TR1.2, TR2, TR2.5 and TR3 are listed in Table 5.6. Model results show that the mean mortality rate of adult in November-April in TR3 is much larger than that in TR1.2. The high mortality rate of adult in winter greatly reduces the abundance of the overwintering adults. The abundance of the overwintering stocks is an important factor determining the seasonal

variation of copepod abundance. *Acartia clausi* in the North Sea overwinters mainly by adults. If the abundance of the overwintering adult is diminished too much in the winter, there will not be enough adults to initialize the new seasonal cycle.

Parameters	mean AMR November-April	mean AMR May-October
TR0	$3.62\%d^{-1}$	$3.58\%d^{-1}$
TR1.2	$3.62\%d^{-1}$	$3.62\%d^{-1}$
TR2	$3.71\%d^{-1}$	$3.97\%d^{-1}$
TR2.5	$4.05\%d^{-1}$	$4.06\%d^{-1}$
TR3	$46.40\%d^{-1}$	$8.48\%d^{-1}$

Table 5.6: The mean Adult Mortality Rate (AMR) in November-April and May-October from TR0, TR1.2, TR2, TR2.5 and TR3

5.5 Discussion

This chapter focuses on the interaction between phytoplankton and *Acartia clausi* in a warmer environment. The increase in the sea temperature changes the phenology of phytoplankton and *Acartia clausi* by directly influencing their physiological processes.

The model results show that when the annual mean SST is increased by 1.2°C compared to the current level, the timing of the maximum phytoplankton biomass concentration is advanced by 8 days. The advance in the timing of the phytoplankton bloom due to climate variations is recorded in previous studies. Edwards and Richardson (2004) compiled the time series data of 66 plankton taxa during the period from 1958-2002 measured in the North Sea and found that over the past 45 years, dinoflagellates in the North Sea were peaking earlier by 23 days. Winder et al. (2012) studied the shifts in the timing of the spring phytoplankton bloom in response to climate warming by cultivating phytoplankton in different sea temperatures in laboratory experiments and found that higher water temperatures advanced the bloom of the most functional phytoplankton groups in marine ecosystems. The model results also show that when temperature rises, the phytoplankton biomass concentration increases. The potential influence of climate warming on the phytoplankton production has been investigated in previous studies. Gregg et al. (2005) reported that since the early 1980s, the global chlorophyll concentration has been increased by 4% corresponding to an increase of 1°C

in SST. Sarmiento et al. (2004) projected using an empirical model that there would be a general increase in chlorophyll concentration in Atlantic Ocean due to future climate warming. Richardson and Schoeman (2004) studied the relationship between SST and the phytoplankton production in the northeastern Atlantic Ocean and found a positive relationship of SST and the phytoplankton concentration in high latitude. From these studies, the projected responses of phytoplankton to future climate warming are reasonable.

In the current study, the response of phytoplankton to climate warming is projected by including all algae species into one model compartment. I have not considered the life cycles of different algae species. But in reality, the life cycles of different algae species are diverse and complex. Different algae species depend on different nutrients and the mechanism regulating the development of their biomass are different. The current study can only provide a rough pattern about the responses of phytoplankton to climate warming.

Acartia clausi functions as grazers in the ecosystem. It is more sensitive and vulnerable to climate warming than phytoplankton. The model results show that when the annual mean sea surface temperature is increased by 1.2°C compared to the current level, the growing season of *Acartia clausi* will be extended and there will be a better temporal match between phytoplankton and *Acartia clausi*. As a consequence, the abundance of *Acartia clausi* increases. The beneficial effects of the climate variation on *Acartia spp.* was observed in the central Baltic Sea (Alheit et al., 2005). The index of the North Atlantic Oscillation (NAO), which is the dominant mode of the climate variation in the North Atlantic region, changed in the 1980s from negative phase to positive phase. The shift of NAO led to an increase in the sea temperature in the central Baltic Sea, which further led to an extended growing season of phytoplankton and *Acartia spp.*. *Acartia spp.* were found to be persistent abundant. The increase in the North Sea *Acartia clausi* abundance might affect the upper trophic level. *Acartia clausi* is reported to be a food source for sprat (Porumb, 1973). When the abundance of *Acartia clausi* is increased in the North Sea, it is very likely that the abundance of sprat will correspondingly increase. In the central Baltic Sea, it is observed that due to increased *Acartia spp.* abundance, sprat abundance increases (Alheit et al., 2005).

When the annual mean SST is increased by more than 2°C, the model projects

that the abundance of *Acartia clausi* will be greatly reduced. The rising sea temperature disturbs the temporal match between phytoplankton and *Acartia clausi*. The rising sea temperature increases the excretion rate of overwintering adults but at the same time, the phytoplankton biomass concentration is not able to increase synchronously because of the light limitation in winter. The combined effect of the high excretion and the food deficiency leads to a high mortality rate of overwintering adults through the starvation effect. The model result that the rising temperature will cause a temporal mismatch between phytoplankton and *Acartia clausi* is obtained because the starvation is parametrized in the model as a death inducing factor. The model result shows that in the conditions with high temperature and low food concentration the mortality rates of *Acartia clausi* are high. This model result is in agreement with the laboratory experimental data from Klein Breteler and Schogt (1994). The decrease in the abundance of *Acartia clausi* may reduce the food availability of sprat and further cause changes in the higher trophic levels. In the North Sea, because of the decrease in *Calanus finmarchicus* abundance since the late 1980s, the cod recruitment has plummeted.

This study is conducted with a one dimensional column model. The horizontal advection of physical and biological variables are not considered. One effect of climate warming on oceans is to alter the large-scale ocean circulation pattern (Richardson, 2008). When taking the horizontal advection into consideration, the response of *Acartia clausi* and phytoplankton to climate warming could be much more complicated. Thus, given all the uncertainties, the results from the present study can not provide a precise estimate about the changes in the abundance of *Acartia clausi* in the future but can present the trend of changes. The projected responses of *Acartia clausi* and phytoplankton to future climate warming are supposed to happen, whereas more sophisticated research tools (general circulation models) are needed for a better prediction of the consequence.

5.6 Summary

In this chapter, firstly I use *Acartia clausi* life cycle model to reproduce the observed seasonal variation of *Acartia clausi* abundance at the Stonehaven sampling station in order to study the life cycle dynamics of this species in the North Sea. The seasonal cycle of *Acartia clausi* shows a marked seasonality in reproduction. In winter, due

to the insufficient food supply, the abundance of *Acartia clausi* is very low and the reproductive activity of the overwintering adults ceases. In May, the overwintering adults begin to produce the first egg cohort when the increase in the phytoplankton biomass concentration can supply sufficient food. The adults produce eggs intensively and successively during the short breeding season from March to June. Several *Acartia clausi* cohorts are thus produced during a short time and the developments of different cohorts overlap with each other. When most of the individuals of the first several generations have developed to the adulthood, the adult abundance reaches its maximum peak of the year. From August, the abundance of *Acartia clausi* begins to decrease due to the food deficiency. In later November, the abundance of *Acartia clausi* has decreased to a very low level. The pattern of the seasonal cycle of *Acartia clausi* in the North Sea fits the general pattern of the seasonal cycle of copepods in temperate waters described in Mauchline (1998).

Next, the potential responses of phytoplankton and *Acartia clausi* to future climate warming are projected. The results show that when the annual mean SST is increased by 1.2°C compared to the current level, the higher temperature leads to a better match between *Acartia clausi* and phytoplankton. Consequently, the abundance of *Acartia clausi* increases. When the annual mean SST is increased by more than 2°C compared to the current level, the temporal match between *Acartia clausi* and phytoplankton is disturbed. The rising temperature increases the excretion rate of the overwintering adults but at the same time the phytoplankton biomass concentration is low due to the light limitation in winter. Because of starvation, the abundance of the overwintering adults decreases. The abundance of the overwintering stocks is an important factor determining the seasonal variation of copepod abundance. If the abundance of overwintering adults is diminished to a low level, there will not be enough individuals to initialize the new seasonal cycle. As a result, the abundance of *Acartia clausi* drops sharply.

The knowledge obtained from this chapter is helpful for better understanding the mechanism driving the food availability of commercially important fishes and useful for developing a capacity to ultimately forecast the recruitment strength of fishes in a warmer environment.

Chapter 6

Conclusions and outlook

In this thesis, firstly I study the sensitivity of the ontogenetic development of *Acartia clausi* to the variations in the temperature and food concentration at different temperature conditions with a life cycle model. Secondly, I use a coupled biological-physical numerical model to simulate the seasonal variation of *Acartia clausi* abundance under different reproductive patterns in the northern, central and southern North Sea, and compare the model results to observations. Through this, I show in the North Sea which kind of reproductive pattern should be considered when modelling the life cycle dynamics of *Acartia clausi* and what is the possible overwintering strategy of this species. Thirdly, I model the seasonal cycle of *Acartia clausi* in the North Sea through reproducing the observations at the Stonehaven sampling station with the coupled biological-physical numerical model. Finally, I project the potential responses of phytoplankton and *Acartia clausi* to projected North Sea temperature rises with a focus on the potential phenological changes of phytoplankton and *Acartia clausi* and study whether the phenological changes will induce a temporal mismatch between them. This study provides a comprehensive understanding of the life cycle dynamics of *Acartia clausi* in the North Sea and it is the first time that an estimate about the changes in the abundance of *Acartia clausi* in the future is given.

6.1 Main finding

Now I can answer the questions raised in Chapter 1.

How is the sensitivity of the ontogenetic development of *Acartia clausi* to the variations in the temperature and food concentration at different temperature conditions?

The model results show that the ontogenetic development of *Acartia clausi* is more sensitive to variations in temperature and food concentration at lower temperatures than at higher temperatures.

Which reproductive pattern can best explain the observed seasonal variation of *Acartia clausi* abundance and which kind of overwintering strategy of *Acartia clausi* should be considered when modelling the life cycle dynamics of this species in the North Sea?

There are two possibilities for the reproductive pattern and the overwintering strategy of *Acartia clausi* in the North Sea. The first one is that only subitaneous eggs are produced and the overwintering strategy is by adults, and the second one is that both subitaneous eggs and dormant eggs are produced and the overwintering strategy is by adults and dormant eggs. The model results show that when considering the first option, the simulated seasonal variation of *Acartia clausi* abundance is more close to the observations at the Stonehaven sampling station (introduced in Chapter 2). Thus, I conclude that it is not necessary to include the dormant egg production into the life cycle model when modelling the life cycle dynamics of *Acartia clausi* in the North Sea and the overwintering strategy of *Acartia clausi* in the North Sea is by adults.

How does the life cycle dynamics of *Acartia clausi* look like in the North Sea?

The pattern of the seasonal cycle of *Acartia clausi* in the North Sea fits the general pattern of the seasonal cycle of copepods in temperate waters described in Mauchline (1998). The seasonal cycle of *Acartia clausi* shows a marked seasonality in reproduction. In winter, due to the low temperature and insufficient food supply, the abundance of *Acartia clausi* is very low and the reproductive activity of the overwintering adults ceases. In May, the overwintering adults begin to produce the first egg cohort when the increase in the phytoplankton biomass concentration can supply sufficient food. The adults produce eggs intensively and successively during the short breeding season from March to June. Several cohorts are produced during a short time and the developments of different cohorts overlap with each other. When the individuals of the first several

generations reach adulthood, the adult abundance reaches the annual maximum peak. From August onwards, the abundance of *Acartia clausi* begins to decrease due to the food deficiency. In late November, the abundance of *Acartia clausi* has decreased to a low level.

What are the potential responses of phytoplankton and *Acartia clausi* to future climate warming? And what are the mechanisms behind?

In the warming scenario in which the annual mean SST is increased by 1.2°C compared to the current level, the higher temperature advances the seasonalities of phytoplankton and *Acartia clausi*. Both the timing of the maximum phytoplankton biomass concentration peak and the timing of the first egg cohort from *Acartia clausi* are advanced by 8 days. Because the higher temperature extend the growing season of *Acartia clausi*, *Acartia clausi* matches better with phytoplankton than under present environmental conditions. Consequently, the abundance of *Acartia clausi* increases.

In the warming scenarios in which the annual mean SST is increased by more than 2°C compared to the current level, the temporal match between *Acartia clausi* and phytoplankton is disturbed. The rising temperature increases the excretion rate of the overwintering adults but at the same time the phytoplankton biomass concentration remains low due to the light limitation in winter. Because of the starvation, the abundance of the overwintering adults decreases. The abundance of the overwintering stocks is an important factor determining the seasonal variation of *Acartia clausi* abundance. If the abundance of the overwintering adults is diminished to a low level, there will not be enough individuals to initialize the new seasonal cycle. Consequently, the abundance of *Acartia clausi* plummets.

6.2 Outlook

6.2.1 Observations

The Mortality rate is an important parameter regulating the abundance and biomass of *Acartia clausi*. The parametrization of the mortality rate in the ecosystem model is very difficult because the mechanism controlling the variation in the copepod mortality

rate is unclear. A reasonable parametrization of mortality rate is very important for estimating the abundance of the copepod communities with a modelling approach. There are several reasons that could cause death of copepods: disease, starvation and predation by higher trophic levels. The relative importance of these factors varies with seasons, e.g., in autumn the predation by higher trophic levels might induce more death of copepods and in winter starvation might be the main source of death. More observations are needed to understand under which conditions, which factors are more influential and how these factors induce death.

Measurements of the ingestion rate of *Acartia clausi* at the low temperature conditions are rare. The model results show that the timing of the seasonal cycle of *Acartia clausi* is very important for the development of the overall abundance of the year. The seasonal cycle of *Acartia clausi* begins in spring when the water temperature is low. If more observations focusing on the ingestion at low temperatures could be conducted, the information obtained from these observations would be helpful for timing the onset of the seasonal cycle of *Acartia clausi* more precisely.

6.2.2 Future model applications

In the current study, the response of phytoplankton to climate warming is projected by integrating all algae species into one model compartment. In reality, the life cycles of different algae species are diverse and complex. Different algae species depend on different nutrients and the mechanisms regulating the development of their biomass are different. In future studies, it would be necessary and helpful to include the life cycle of the main biomass forming algae species in marine ecosystems into the model.

This study is conducted with a one dimensional water column model. The horizontal advection of physical and biological variables is not considered. One effect of climate warming on oceans is to alter the large-scale ocean circulation pattern (Richardson, 2008). When taking the exchange of biological variables between different regions into account, the responses of *Acartia clausi* and phytoplankton to climate warming could be much more complicated compared to what I have found in this thesis. Thus, in the future it would be necessary to couple the ecosystem model to a three dimensional ocean circulation model.

Appendix A

Summary of the ecosystem model parameters

Parameters	Description	Unit
P	phytoplankton biomass concentration	mmol N m^{-3}
N_u	nutrient concentration	mmol N m^{-3}
Z_1	subitaneous egg biomass concentration	mmol N m^{-3}
Z_2	nauplius biomass concentration	mmol N m^{-3}
Z_3	copepodite biomass concentration	mmol N m^{-3}
Z_4	adult biomass concentration	mmol N m^{-3}
Z_5	immature dormant egg biomass concentration	mmol N m^{-3}
Z_6	mature dormant egg biomass concentration	mmol N m^{-3}
A_1	subitaneous egg abundance	individuals m^{-3}
A_2	nauplius abundance	individuals m^{-3}
A_3	copepodite abundance	individuals m^{-3}
A_4	adult abundance	individuals m^{-3}
A_5	immature dormant egg abundance	individuals m^{-3}
A_6	mature dormant egg abundance	individuals m^{-3}
D_l	large detritus concentration	mmol N m^{-3}
D_s	small detritus concentration	mmol N m^{-3}

Table A.1: The model compartments of the ecosystem model.

Parameters	Description	Unit
μ_P	phytoplankton growth rate	d^{-1}
$\mu_{P_{max}}$	maximum phytoplankton growth rate	d^{-1}
r_{par}	photosynthetically active radiation	W m^{-2}
k_w	absorption coefficient of seawater	m^{-1}
k_c	absorption coefficient of organic matter	m^2 mmol N^{-1}
I_{min}	minimum photosynthetically active radiation	W m^{-2}
I_0	sea surface photosynthetically active radiation	W m^{-2}
k_{N_u}	coefficient for phytoplankton nutrient uptake	mmol N m^{-3}
η_P	phytoplankton mortality rate	d^{-1}
γ	detritus remineralization rate	d^{-1}
l_P	phytoplankton exudation rate	d^{-1}
φ	proportion of small detritus to total detritus	-
w_P	vertical velocity of phytoplankton	m d^{-1}
w_{D_l}	vertical velocity of large detritus	m d^{-1}
w_{D_s}	vertical velocity of small detritus	m d^{-1}
w_{Z_i}	vertical velocities of different life cycle stages	m d^{-1}

Table A.2: A summary of the parameters for the PND compartments.

Parameters	Description	Unit
Ingestion		
g_{i_P}	ingestion rate on phytoplankton	d^{-1}
$g_{i_{D_s}}$	ingestion rate on small detritus	d^{-1}
$g_{i_{\max_P}}$	maximum ingestion rate on phytoplankton	d^{-1}
$g_{i_{D_s}}$	maximum ingestion rate on small detritus	d^{-1}
k_P	half saturation coefficient for ingestion on phytoplankton	mmol N m^{-3}
k_{D_s}	half saturation coefficient for ingestion on small detritus	mmol N m^{-3}
α	power factor for ingestion	-
T_{opt}	optimum temperature for ingestion	°C
T_1	reference temperature for ingestion	°C
T_2	reference temperature for ingestion	°C
W_i	mean individual body weight	mmol N ind^{-1}
W_{min}	minimum individual body weight for ingestion	mmol N ind^{-1}
W_{max}	maximum individual body weight for ingestion	mmol N ind^{-1}

Table A.3: A summary of the parameters for the source term (ingestion) in the life cycle model of *Acartia clausi*.

Parameters	Description	Unit
Egestion and excretion		
β_P	assimilation efficiency for phytoplankton	-
β_{D_s}	assimilation efficiency for small detritus	-
ς_i	excretion rate	d^{-1}
$Q10$	Q10 parameter for excretion	-
T_{ref}	reference temperature for excretion	°C
Mortality		
f_{c_i}	curve factor for body weight dependent mortality rate	-
r_{max}	maximum mortality rate	d^{-1}
r_i	constant mortality rate	d^{-1}
ω_i	switch for body weight dependent mortality rate	-

Table A.4: A summary of the parameters for loss terms in the life cycle model.

Parameters	Description	Unit
Moulting		
$m_{i,j}$	maximum transfer rate	d^{-1}
W_{ref}	reference individual body weight	mmol N ind^{-1}
k_{w_i}	curve factor for moulting	mmol N ind^{-1}
Reproduction		
k_{w_4}	curve factor for reproduction	mmol N ind^{-1}
δ	maximum reproduction rate	d^{-1}
ρ_{fem}	proportion of female adult	-
ε_j	proportion of the dormant egg	-
Hatching and immature dormant egg to mature dormant egg transition		
T_{scale}	reference temperature for hatching	°C
n	curve factor for hatching	$°C^{-1}$
D_{th}	mandatory dormancy period	d

Table A.5: A summary of the parameters for life cycle stage transitions in the life cycle model.

Bibliography

Alheit, J., Möllmann, C., Dutz, J., Kornilovs, G., Loewe, P., Mohrholz, V., and Wasmund, N. (2005). Synchronous ecological regime shifts in the central Baltic and the North Sea in the late 1980s. ICES Journal of Marine Science, 62:1205-1215.

Beaugrand, G., Brander, K. M., Lindley, J. A., Souissi, S., and Reid, P. C. (2003). Plankton effect on cod recruitment in the North Sea. Nature, 426:661-664.

Beaugrand, G. (2009). Decadal changes in climate and ecosystems in the North Atlantic Ocean and adjacent seas. Deep-Sea Research Part II, 56:656-673.

Bakker, C., Tackx, M. L. M., and van Rijswijk, P. (1988). Plankton copepods *Temora longicornis* and *Acartia tonsa* and their food in the Oosterschelde estuary (S.W. Netherlands). Hydrobiology Bulletin, 22:75-78.

Becker, G. A. and Schulz, A. (2000). Atlas of North Sea surface temperatures. Weekly and monthly means for the period 1969 to 1993. Deutsche Hydrographische Zeitschrift, 51:5-79.

Bolding, K., Burchard, H., Pohlmann, T., and Stips, A. (2002). Turbulent mixing in the Northern North Sea: a numerical model study. Continental Shelf Research, 22:2707-2724.

Bradford, J. (1976). Partial revision of the *Acartia* subgenus *Acartiura* (Copepoda: Calanoida: Acartiidae). New Zealand Journal of Marine and Freshwater Research, 10:159-202.

Bresnan, E., Hay, S., Hughes, S. L., Fraser, S., Rasmussen, J., Webster, L., Slesser, G., Dunn, J., and Heath, M. R. (2009). Seasonal and interannual variation in the phytoplankton community in the north east of Scotland. Journal of Sea Research, 61:17-25.

Bresnan, E. (2012). Stonehaven. In: O'Brian, T. D., et al. (Eds.), ICES Phytoplankton and Microbial Plankton Status Report 2009/2010. ICES Cooperative Research Report, 313, 14 pp.

Burchard, H. (1999). Recalculation of surface slopes as forcing for numerical water column models of tidal flow. Journal of Mathematical Modelling and Application, 23:737-755.

Bělehrádek, J. (1935). Temperature and living matter. Berlin, Gebrüder Bornträger, Protoplasma Monography No. 8, 277 pp.

Chen, X., Liu, C., O'Driscoll, K., Mayer, B., Su, J., and Pohlmann, T. (2012). On the nudging terms at open boundaries in regional ocean models. Ocean Modelling, 66:14-25.

Cheng, Y., Canuto, V. M., and Howard, A. M. (2002). An improved model for the turbulent PBL. Journal of Atmospheric Science, 59:15501565.

Colebrook, J. M. (1982). Continuous plankton records: persistence in time-series and the population dynamics of *Pseudocalanus elongatus* and *Acartia clausi*. Marine Biology, 66: 289-294.

Dagg, M. J. (1977). Some effects of patchy food environments on copepods. Limnology and Oceanography, 22:99-107.

Dahms, H. U. (1995). Dormancy in the Copepods - an overview. Hydrobiologia, 306:199-211.

De Wilde, P. A. W. J., Jenness, M. I., and Duineveld, G. C. A. (1992). Introduction into the ecosystem of the North Sea: hydrography, biota, and food web relationship. Netherlands Journal of Aquatic Ecology, 26:7-18.

Ducklow, H. W., Steinberg, D. K., and Buesseler K. O. (2001). Upper ocean carbon export and the biological pump. Oceanography, 14:50-58.

Eisma, D. (1987). The North Sea, an overview. Philosophical Transactions of the Royal Society B, 316:461-485.

Engel, M., and Hirche, H. J. (2004). Seasonal variability and inter-specific differences in hatching of calanoid copepod resting eggs from sediments of the German Bight (North Sea). Journal of Plankton Research, 26:1083-1093.

Edwards, M., and Richardson, A. J. (2004). The impact of climate change on the phenology of the plankton community and trophic mismatch. Nature, 430:881-884.

Eppley, R. W. (1972). Temperature and phytoplankton growth in the sea. Fishery Bulletin, 70:1063-1085.

Fennel, W. (2001). Modelling of copepods with links to circulation models. Journal of Plankton Research, 23:1217-1232.

Fisheries Research Services (2003). Scottisch Ocean Climate Status Report 2001 and 2002, In: Hughes, S. L. (Eds.). Aberdeen, Fisheries Research Services Internal Report, 22 pp.

Fransz, H. G., and Gieskes, W. W. C. (1984). The unbalance of phytoplankton and copepods in the North Sea. ICES Journal of Marine Science, 183:218-225.

Fransz, H. G., Colebrook, J. M., Gamble, J. C., and Krause, M. (1991). The zooplankton of the North Sea. Netherlands Journal of Sea Research, 28:1-52.

Fransz, H. G., Gonzalez, S. R., and Steeneken, S. F. (1998). Metazoan plankton and the structure of the plankton community in the stratified North Sea. Marine Ecology Progress Series, 175:191-200.

Gaudy, R., Cerretto, G., and Pagano, M. (2000). Comparison of the metabolism of *Acartia clausi* and *A. tonsa*: influence of temperature and salinity. Journal of Experimental Marine Biology and Ecology, 247:51-65.

Geider, R., and Roche, J. (2002). Redfield revisited: variability of C:N:P in marine microalgae and its biochemical basis. European Journal of Phycology, 37:1-17.

Glover, R. S. (1957). An ecological survey of the drift-net Herring fishery off the north-east coast of Scotland. Part II. The planktonic environment of the Herring. Bulletin of Marine Ecology, 5:1-43.

Gordon, C., Cooper, C., Senior, C. A., Banks, H., Gregory, J. M., Johns, T. C., Mitchell, J. F. B., and Wood, R. A. (2000). The simulation of SST, sea ice extents and ocean heat

transports in a version of the Hadley Centre coupled model without flux adjustments. Climate Dynamics, 16:147168.

Gregg, W. W., Casey, N. W., and McClain, C. R. (2005). Recent trends in global ocean chlorophyll. Geophysical Research Letters, 32, L03606, doi:10.1029/2004GL021808.

Grice, G. D., and Marcus, N. H. (1981). Dormant eggs of marine copepods. Oceanography and Marine Biology: An Annual Review, 19:125-140.

Hay, S. J., Evans, G. T., and Gamble, J. C. (1988). Birth, growth and death rates for enclosed populations of calanoid copepods. Journal Plankton Research, 10:431-454.

Hense, I., and Beckmann, A. (2010). The representation of cyanobacteria life cycle processes in aquatic ecosystem models. Ecological Modelling, 221:2330-2338.

Holling, C. S. (1965). The influence response of predators to prey density and its role in mimicry and population regulation. Memoirs of the Entomological Society of Canada, 45:3-60.

Hu, S. M., Liu, S., Li, T., and Guo, Z. L. (2012). Advances in feeding ecology of *Acartia*. Acta Ecologica Sinica, 32:5870-5877.

Huntley, M. E., and Lopez, M. D. G. (1992). Temperature-Dependent Production of Marine Copepods: A Global Synthesis. The American Naturalist, 140:201-242.

IPCC (2007). Climate Change 2007 - The physical Basis. In Solomon, S., et al. (Eds.), Contribution of Working Group I to the Fourth Assessment Report of the IPCC. Cambridge, Cambridge University Press, 996 pp.

Janssen, F., Schrum, C., and Backhaus, J. O. (1999). A climatological data set of temperature and salinity for the Baltic Sea and the North Sea. Deutsche Hydrographische Zeitschrift, 51:5-245, 1999.

Kalnay, E., Kanamitsu, M., Kistler, R., Collins, W., Deaven, D., Gandin, L., Iredell, M., Saha, S., White, G., Woollen, J., Zhu, Y., Leetmaa, A., and Reynold, R. (1996). The NCEP/NCAR 40-year reanalysis project. Bulletin of the American Meteorological Society, 77:437-470.

Katechakis, A., Stibor, H., Sommer, U., and Hansen, T. (2004). Separation of *Acartia clausi, Penilia avirostris* (Crustacea) and *Doliolum denticulatum* (Thaliacea) in Blanes Bay (Catalan Sea, NW Mediterranean). Journal of Plankton Research, 26:589603.

Kleiber, M. (1961). The fire of life: an introduction to animal energetics. New York, John Wiley & Sons Incorporation, 545 pp.

Klein Breteler, W. C. M., and Gonzalez, S. R. (1982). Influence of cultivation and food concentration on body length of calanoid copepods. Marine Biology, 71:157-161.

Klein Breteler, W. C. M., and Schogt, N. (1994). Development of *Acartia clausi* (Copepoda, Calanoida) cultured at different conditions of temperature and food. Hydrobiologia, 292/293:469-479.

Kondo, J. (1975). Air-sea bulk transfer coefficients in diabatic conditions. Boundary Layer Meteorology, 9:91112.

Kühn, W., and Radach, G. (1997). A one-dimensional physical-biological model study of the pelagic nitrogen cycling during the spring bloom in the northern North Sea (flex76). Journal of Marine Reasearch, 55:687-734.

Levitus, S., Antonov, J. I., Boyer, T. P., and Stephens, C. (2000). Warming of the world ocean. Science, 287:2225-2229.

Lindley, J. A. (1990). Distribution of overwintering calanoid copepod eggs in sea-bed sediments. Marine Biology, 104:209-217.

Lindley, J. A., Gamble, J. C., and Hunt, H. G. (1995). A change in the zooplankton of the central North Sea (55-58°N): a possible consequence of changes in the benthos. Marine Ecology Progress Series, 119:299-303.

Lynch, M. (1983). Estimation of size-specific mortality rates in zooplankton populations by periodic sampling. Limnology Oceanography, 28:533-545.

Mackas, D. L., Goldblatt, R., and Lewis, A. G. (1998). Interdecadal variation in development timing of *Neocalanus plumchrus* populations at Ocean Station P in the Subarctic North Pacific. Canadian Journal of Fisheries and Aquatic Sciences, 55:1878-1893.

Marcus, N. H. (1996). Ecological and evolutionary significance of resting eggs in marine copepods: Past, present, and future studies. Hydrobiologia, 320:141-152.

Mauchline, J. (1998). The biology of calanoid copepods. New York, Academic Press, 710 pp.

Mayzaud, P., Tirelli, V., Bernard, J., and Mayzaud, O. (1998). The influence of food quality on the nutritional acclimation of the copepod *Acartia clausi*. Journal of Marine System, 15:483-493.

McLaren, I. A., Corkette, C. J., and Zillioux, E. J. (1969). Temperature adaptation of copepods eggs from the Arctic to the tropics. Biology Bulletin, 137:486-493.

McLaren, I. A. (1978). Generation lengths of some temperate marine copepods: estimation, prediction and implications. Journal Fisheries Research Board Canada, 35:1330-1342.

McLaren, I. A. (1986). Is "structural" growth of *Calanus* potentially exponential?. Limnology and Oceanography, 31:1342-1346.

Möllmann, C., Müller-Karulis, B., Kornilovs, G., and St. John, M. A. (2008). Effects of climate and overfishing on zooplankton dynamics and ecosystem structure: regime shifts, trophic cascade, and feedback loops in a simple ecosystem. ICES Journal of Marine Science, 65:302-310.

Nielsen, T. G., and Munk, P. (1998). Zooplankton diversity and the predatory impact by larval and small juvenile fish at the Fisher Banks in the North Sea. Journal of Plankton Research, 20:2313-2332.

Open Government Licence (2013): `http://www.nationalarchives.gov.uk/doc/open-government-licence/version/1/`; accessed November 29., 2013.

Otto, L., Zimmermann, J. T. F., Furnes, G. K., Mork, M., Saetre, R., and Becker, G. (1990). Review of the physical oceanography of the North Sea. Netherlands Journal of Sea Research, 26:161-238.

Planque, B., and Fromentin, J. M. (1996). *Calanus* and environment in the eastern North Atlantic .I. Spatial and temporal patterns of *C. finmarchicus* and *C. helgolandicus*. Marine Ecology Progress Series, 134:101-109.

Pope, J. G., and Macer, C. T. (1996). An evaluation of the stock structure of North sea cod, haddock and whiting since 1920, together with a consideration of the impacts of fisheries and predation effects on their biomass and recruitment. ICES Journal of Marine Science, 53:1157-1169.

Porumb, L. I. (1973). Role de Sprattus sprattus (Linne, 1758) dans I'utilisation du zooplancton des eaux Roumaines de la Mer Noire. Revue des Travaux de I'Institut des Pêches Maritimes, 37:203-205.

Radach, G., and Pätsch, J. (1997). Climatological annual cycles of nutrients and chlorophyll in the North Sea. Journal of Sea Research, 38:231-248.

Rae, K. M., and Rees, C. B. (1947). Continuous plankton records: the Copepoda of the North Sea, 1938-1939. Hull Bulletin of Marine Ecology, 2:95-133.

Reid, P. C., Lancelot, C., Gieskes, W. W. C., Hagmeier, E., and Weickart, G. (1990). Phytoplankton of the North Sea and its dynamics: a review. Netherlands Journal of Sea Research, 26:295-331.

Reid, P. C., Edwards, M., Beaugrand, G., Skogen, M. and Stevens, D. (2003). Periodic changes in the zooplankton of the North Sea during the twentieth century linked to oceanic inflow. Fisheries Oceanography, 12:260-269.

Richardson, A. J., and Schoeman, D. S. (2004). Climate impact on plankton ecosystems in the Northeast Atlantic. Science, 305:1609-1612.

Richardson, A. J. (2008). In hot water: zooplankton and climate change. ICES Journal of Marine Science, 65:279-295.

Rodi, W. (1987). Examples of calculation methods for flow and mixing in stratified fluids. Journal of Geophysical Research, 92:53055328.

Sarmiento, J. L., Slater, R., Barber, R., Bopp, L., Doney, S. C., Hirst, A. C., Kleypas, J., Matear, R., Mikolajewicz, U., Monfray, P., Soldatov, V., Spall, S. A., and Stouffer, R. (2004). Response of ocean ecosystem to climate warming. Global Biogeochemical Cycles, 18, GB3003, doi:10.1029/2003GB002134.

Schumann, U., and Gerz, T. (1995). Turbulent mixing in stably stratified shear flows. Journal of Applied Meteorology, 34:33-48.

Sichlau, M. H., Hansen, J. L. S., Andersen, T. J., and Hansen, B. W. (2011). Distribution and mortality of diapause eggs from calanoid copepods in relation to sedimentation regimes. Marine Biology, 158:665-676.

Smetacek, V. (1984). The supply of food to the benthos. In: Fasham, M. J. R. (Eds.), Estuaries and coasts; spatial and temporal theory and practice. New York, Plenum Press, 517 pp.

Steele, J. H. (1974). The structure of marine ecosystem. Oxford, Blackwell, 128 pp.

Stegert, C., Kreus, M., Carlotti, F., and Moll, A. (2007). Parametrization of a zooplankton population model for *Pseudocalanus elongatus* using stage durations from laboratory experiments. Ecological Modelling, 206:213-230.

Sullivan, B., and McManus, L. (1986). Factors controlling seasonal succession of the copepods *Acartia hudsonica* and *A. tonsa* in Narragansett Bay, Rhode Island: temperature and resting egg production. Marine Ecology Progress Series, 28:121-128.

Threlkeld, S. T. (1976). Starvation and size structure of zooplankton communities. Freshwater Biology, 6:489-496.

Tiselius, P. (1989). Contribution of alorocate ciliates to the diet of *Acartia clausi* and *Centropages hamatus* in coastal waters. Marine Ecology Progress Series, 56:49-56.

Thomas, M. K., Kremer, C. T., Klausmeier, C. A., and Litchman, E. (2012). A global pattern of thermal adaptation in marine phytoplankton. Science, 338:108-109.

McGill, R., Tukey, J. W., and Larsen, W. A. (1978). Variation of Box Plots. The American Statistician, 32:12-16.

Turrell, W. R., Henderson, E. W., Slesser, G., Payne, R., and Adams, R. D. (1992). Seasonal changes in the circulation of the northern North Sea. Continental Shelf Research, 12:257-286.

Umlauf, L., Burchard, H. and Bolding, K. (2005). General Ocean Turbulence Model. Scientific documentation. v3.2. Marine Science Reports 63, Baltic Sea Research Institute Warnemünde, Warnemünde, Germany.

Uye, S. (1980). Development of neritic copepods *Acartia clausi* and *A. steuri*. I. Some environmental factors affecting egg development and the nature of resting eggs. Bulletin of Plankton Society of Japan, 27:1-9.

Uye, S. (1981). Fecundity studies of neritic calanoid copepods *Acartia clausi* Giesbrecht and *A. Steueri* Smirnov: A simple empirical model of daily egg production. Journal of Experimental Marine Biology and Ecology, 50:255-271.

Uye, S. (1985). Resting egg production as a life history strategy of marine planktonic copepods. Bulletin of Marine Science, 37:440-449.

Warns, A., Inga, H., and Kremp, A. (2013). Modelling the life cycle of dinoflagellates: a case study with *Biecheleria baltica*. Journal Plankton Research, 35:379-392.

Wesche, A., Wiltshire, K. H., and Hirsche, H. J. (2007). Overwintering strategies of dominant calanoid copepods in the German Bight, southern North Sea. Marine Biology, 151:1309-1320.

White, J. R., and Roman, M. (1992). Seasonal study of grazing by metazoan zooplankton in the mesohaline Chesapeake Bay. Marine Ecology Progress Series, 86:251-261.

Winder, M., Berger, S. A., Lewandowska, A., Aberle, N., Lengfellner, K., Sommer, U., and Diehl, S. (2012). Spring phenological responses of marine and freshwater plankton to changing temperature and light conditions. Marine Biology, 159:2491-2501.

Acknowledgements

It is hard to believe how fast the time elapses. More than three years have passed since the first time I arrived at Hamburg from Shanghai. I still remember the day that Inga picked me up from the Hamburg Airport. Her smiles greatly relieved the pressure I felt when the first time I came to a totally new environment. Now when I think about that scene, I feel that it happened just yesterday. The memory is still so fresh to me. In the next few days, Matthias led me to different offices and helped me to get all the documents, such as work contract, visa, etc and Inga introduced me to the colleagues in the institute. I felt I was settling down.

Working in Germany has been a great and inspiring experience. I have learned a lot about ecosystem and ecosystem modelling, and developed a cool model about *Acartia clausi* and have many ideas for what to do in the next steps. I have fought many bloody battles with Fortran and matlab and luckily won them all. I have learned to speak German, travelled a lot around Europe and experienced different new things, e.g., living in the hospital for two weeks. Eventually, the most valuable treasure I get from the three years is that I have met so many wonderful persons. Many years from now, when I think about this time before going to bed, I would feel lucky that I made the decision to come to Hamburg to do this PhD.

And now, I have finally finished this thesis. The first person I would like to thank is Prof. Dr. Inga Hense. Without her excellent guide, I wouldn't finish this work. Thanks, Inga. You have always been supportive and given me a lot of good advices.

I would also like to thank the other members of my advisory panel, Prof. Dr. Carsten Eden and Prof. Dr. Marc Hufnagl for their time and fruitful discussions.

May the happiness always be with my fellow office mates, Dr. Sebastian Sonntag and Dr. Alexandra Warns. It is a great pleasure to be in the same office with you.

Especially, I would like to thank Dr. Sebastian Sonntag for the helpful advices in thesis writing and the professional translation of the abstract from English into German.

Another big thank goes to Dr. Eileen Bresnan and Ms Tracy McCollin from Fisheries Research Services Marine Laboratory, Aberdeen, UK for sending me the high quality observation data at the Stonehaven sampling station. Without these data, I would not be able to finish this thesis at all.

I am thankful to the colleagues in IHF, Hamburg University for their encouraging support, Dr. Rolf Koppelmann, Dr. Emmanuel Acheampong, Dr. Klas Ove Möller, Dr. Rabea Diekmann and Prof. Dr. Christian Möllmann.... The suggestions from you are really helpful. I would like to thank Xinping Chen from ZMAW for the temperature and salinity data and Peter Damm for preparing NCEP/NCAR data and Dr. Jian Su for constructive suggestions in thesis writing.

I also want to thank the SICSS (and the German taxpayers) for financial support.

I am very grateful for my family, especially my parents and grandparents. You brought me up and shaped me into the person I am. You have supported me when I decided to go to Germany for studying, although you could not understand why I wanted to quit the job in Hangzhou and go abroad to do something as crazy as a PhD.

Eidesstattliche Erklärung

Ich erkläre hiermit an Eides statt, dass ich

- die vorliegende Dissertationsschrift selbst verfasst habe,
- keine anderen als die von mir angegebenen Quellen und Hilfsmittel benutzt habe.

Hamburg, den 11 September 2013 Chuanxi Xing